Scheme 2. Solid-Phase Synthesis of *PBX*-ODNs using *PBH*-ODNs 4 and 5 As Precursors[a]

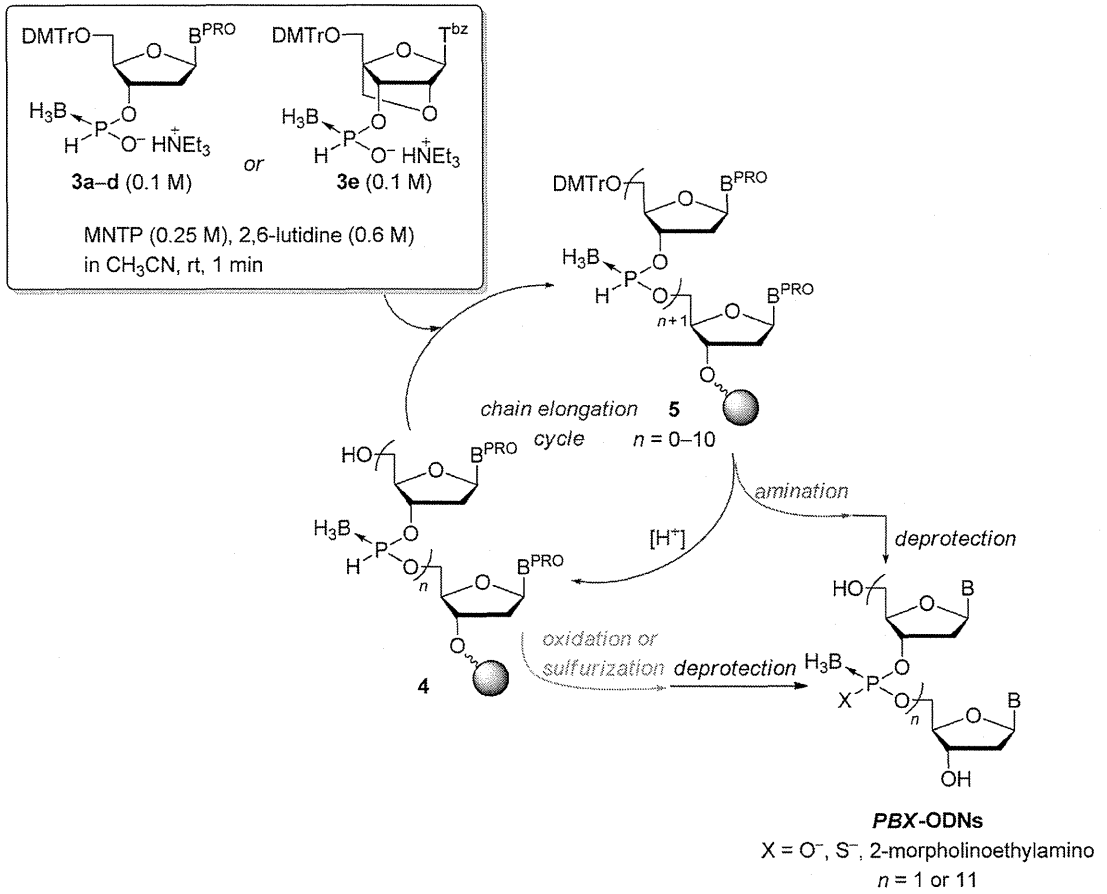

[a]Detritylation: 3% dichloroacetic acid (DCA) in CH_2Cl_2–Et_3SiH (1:1, v/v), rt, 30 s; oxidation: *i*-Pr_2NEt, CCl_4, H_2O in CH_3CN, rt, 30 min; sulfurization: *i*-Pr_2NEt, *N,N'*-dimethylthiuram disulfide (DTD) in CH_3CN, rt, 1 h; amination: CCl_4, 4-(2-aminoethyl)morpholine in CH_3CN, rt, 30 min.

Scheme 3. Plausible Mechanisms of Conversions

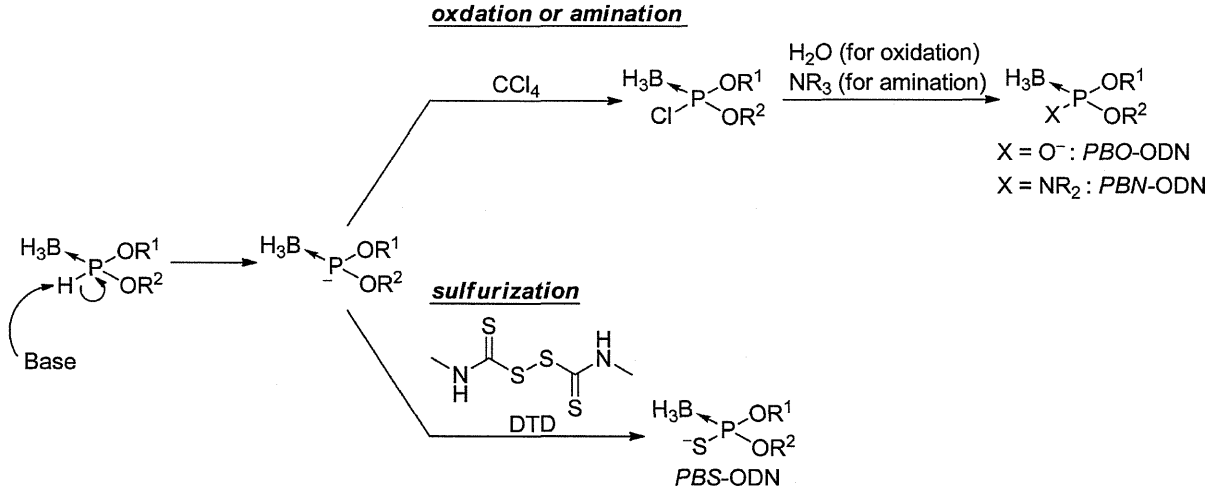

aminoethyl)morpholine (Scheme 3, amination).[18,21] Reversed-phase HPLC (RP-HPLC) analysis of the crude mixtures showed that the desired *PBX*-ODN 2mers were obtained in 94–98% yields without any side reactions (Table 2).[23] Notably, the boranophosphate (*PBO*) and boranophosphorothioate (*PBS*) diesters were susceptible to $DMTr^+$, even in the presence of Et_3SiH.[20] Therefore, as shown in Scheme 2, the 5′-detritylation step had to be performed prior to the *P*-modification (oxidation or sulfurization) step for the synthesis of the *PBO* and *PBS*-ODN 2mers. In contrast, the

dx.doi.org/10.1021/jo500185b | J. Org. Chem. 2014, 79, 3465–3472

Table 2. Solid-Phase Synthesis of *PBO*, *PBS*, and *PBN*-ODN 2mers

entry	monomer (B^{PRO})	*P*-modification	product[a]	yield [%][b]
1	**3a** (T^{bz})	oxidation	$T_{PBO}T$ (**6a**)	96
2	**3b** (A^{bz})	oxidation	$dA_{PBO}T$ (**6b**)	96
3	**3c** (C^{ibu})	oxidation	$dC_{PBO}T$ (**6c**)	95
4	**3d** ($G^{ce,\ ibu}$)	oxidation	$dG_{PBO}T$ (**6d**)	97
5	**3a** (T^{bz})	sulfurization	$dT_{PBS}T$ (**7a**)	98
6	**3b** (A^{bz})	sulfurization	$dA_{PBS}T$ (**7b**)	96
7	**3c** (C^{ibu})	sulfurization	$dC_{PBS}T$ (**7c**)	97
8	**3d** ($G^{ce,\ ibu}$)	sulfurization	$dG_{PBS}T$ (**7d**)	98
9	**3a** (T^{bz})	amination[c]	$T_{PBN}T$ (**8**)	96
10	**3a** (T^{bz})	amination[d]	$T_{PBN}T$ (**8**)	94

[a]Subscript 'PBO', 'PBS', and 'PBN' = boranophosphate diester, boranophosphorothioate diester, and *N*-(2-morpholinoethyl) boranophosphoramidate diester, respectively. [b]Determined by RP-HPLC. [c]Amination was performed prior to 5′-detritylation. [d]Amination was performed after 5′-detritylation.

boranophosphoramidate linkage of the *PBN*-ODN was less susceptible to $DMTr^+$; thus, the amination step for the synthesis of the *PBN*-ODN 2mer could be performed either before or after the 5′-detritylation, although a slightly better yield was obtained when the amination was performed prior to the 5′-detritylation (Table 2, entry 9 vs entry 10).

Next, using the optimized conditions, we synthesized *PBX*-ODN 12mers **9**–**14** (Table 3) bearing backbones thoroughly

Table 3. *PBX*-ODN 12mers 9–14 Synthesized *via* *PBH*-ODNs

PBX-ODN	yield [%][b]
$T(_{PBO}T)_{11}$ (**9**)	28
$T(_{PBS}T)_{11}$ (**10**)	31
$T(_{PBN}T)_{11}$ (**11**)	10
$G_{PBO}C_{PBO}A_{PBO}T_{PBO}T_{PBO}G_{PBO}G_{PBO}T_{PBO}A_{PBO}T_{PBO}T_{PBO}C$ (**12**)	44
$G_{PBS}C_{PBS}A_{PBS}T_{PBS}T_{PBS}G_{PBS}G_{PBS}T_{PBS}A_{PBS}T_{PBS}T_{PBS}C$ (**13**)	16
$G_{PBO}C_{PBO}A_{PBO}T^{L}_{PBO}T^{L}_{PBO}G_{PBO}G_{PBO}T^{L}_{PBO}A_{PBO}T^{L}_{PBO}T^{L}_{PBO}C$ (**14**)[a]	7

[a]T^L = LNA thymidine. [b]Isolated yield.

modified with boranophosphate diesters (*PBO*-ODNs **9**, **12**, **14**), boranophosphorothioate diesters (*PBS*-ODNs **10**, **13**), or *N*-(2-morpholinoethyl)boranophosphoramidate diesters (*PBN*-ODN **11**) according to Scheme 2. An antisense sequence against apoB protein mRNA[24] (5′-GCA TTG GTA TTC-3′) was chosen for the *PBX*-ODNs **12**–**14**. We also synthesized a *PBO*-ODN wherein all the thymidine 3′-boranophosphate moieties were replaced with LNA thymidine 3′-boranophosphates (^{LNA}*PBO*-ODN **14**) by using LNA thymidine monomer **3e**.[25]

Hybridization Properties of *PBX*-ODNs. Finally, the hybridization properties of *PBX*-ODN 12mers **9**–**14** with complementary ODNs and oligoribonucleotides (ORNs) were examined. Melting temperatures (T_m) for the duplexes of the homothymidylate 12mers **9**–**11** with the complementary dA_{12} and rA_{12} could not be determined.[23] In contrast, the 12mers containing all four nucleobases **12**–**14** formed duplexes with the complementary ODN and ORN (Table 4, Figures 1 and 2). On the basis of the T_m values of 2′-deoxy ODNs (Table 4, entries 1–4), the order of duplex stability is natural ODN **15**, *PS*-ODN **16**, *PBO*-ODN **12**, and *PBS*-ODN **13**. These results suggest that the hydrophobic and sterically hindered groups

Table 4. T_m Values of the Duplexes of ODNs with Complementary ODN and ORN

		complementary strand	
		ODN[b]	ORN[c]
entry	oligonucleotide[a]	T_m [°C] (ΔT_m [°C], ΔT_m/mod. [°C])	T_m [°C] (ΔT_m [°C], ΔT_m/mod. [°C])
	0.1 M NaCl, 10 mM NaH_2PO_4–Na_2HPO_4, pH 7.0		
1	natural ODN (**15**)	42.7	42.0
2	*PS*-ODN (**16**)	31.3 (-11.4^d, -1.0^e)	32.2 (-9.8^d, -0.9^e)
3	*PBO*-ODN (**12**)	25.9 (-16.8^d, -1.5^e)	29.9 (-12.1^d, -1.1^e)
4	*PBS*-ODN (**13**)	15.7 (-27.0^d, -2.5^e)	25.0 (-17.0^d, -1.5^e)
5	^{LNA}*PO*-ODN (**17**)	60.1 ($+17.4^d$, $+3.5^f$)	69.0 ($+27.0^d$, $+5.4^f$)
6	^{LNA}*PS*-ODN (**18**)	54.6 (-5.5^g, -0.5^h)	64.2 (-4.8^g, -0.4^h)
7	^{LNA}*PBO*-ODN (**14**)	52.1 (-8.0^g, -0.7^h)	63.9 (-5.1^g, -0.5^h)

[a]Natural ODN **15**: $G_{PO}C_{PO}A_{PO}T_{PO}T_{PO}G_{PO}G_{PO}T_{PO}A_{PO}T_{PO}T_{PO}C$; *PS*-ODN **16**: $G_{PS}C_{PS}A_{PS}T_{PS}T_{PS}G_{PS}G_{PS}T_{PS}A_{PS}T_{PS}T_{PS}C$; ^{LNA}*PO*-ODN **17**: $G_{PO}C_{PO}A_{PO}T^{L}_{PO}T^{L}_{PO}G_{PO}G_{PO}T^{L}_{PO}A_{PO}T^{L}_{PO}T^{L}_{PO}C$; ^{LNA}*PS*-ODN **18**: $G_{PS}C_{PS}A_{PS}T^{L}_{PS}T^{L}_{PS}G_{PS}G_{PS}T^{L}_{PS}A_{PS}T^{L}_{PS}T^{L}_{PS}C$. [b]3′-CGT AAC CAT AAG-5′. [c]3′-CGU AAC CAU AAG-5′. [d]Difference from the T_m of natural ODN/ODN (ORN). [e]Difference of the T_m values per *PS*, *PBO*, or *PBS* linkage. [f]Difference of the T_m values per LNA thymidine. [g]Difference from the T_m of ^{LNA}*PO*-ODN/ODN (ORN). [h]Difference of the T_m values per *PS* or *PBO* linkage.

destabilize the duplex. However, notably, the *PBX*-ODN 12mers **12** and **13** formed more stable duplexes with ORN than with ODN, indicating that the *PBX*-backbones generally favor the duplex formation with complementary ORNs rather than ODNs, which would be advantageous for antisense strategy.[10b,26]

The duplex stability of ^{LNA}*PBO*-ODN **14** was comparable with that of ^{LNA}*PS*-ODN **18** (Table 4, entry 6 vs 7). Although the T_m value of ^{LNA}*PBO*-ODN **14** was lower than that of ^{LNA}*PO*-ODN **17**, the difference of the T_m values was 5.1–8.0 °C (Table 4, entry 5 vs 7). On the other hand, the difference of the T_m values of 2′-deoxy natural ODN **15** and *PBO*-ODN **12** was 12.1–16.8 °C (Table 4, entry 1 vs 3). These results suggest that the incorporation of LNA can make up for the reduction of the duplex stability caused by the BH_3 group. Thus, because ^{LNA}*PBO*-ODN **14** showed a significantly enhanced affinity to the complementary strands, it has a great potency as an antisense therapeutic oligonucleotide.

■ CONCLUSION

In conclusion, we developed *H*-boranophosphonate oligonucleotide and demonstrated its versatility as a precursor to various *PBX*-ODNs. By using the *H*-boranophosphonate method, incorporation of LNA to the oligomers can be performed easily. Therefore, the present approach is efficient for the synthesis of versatile antisense molecules. The *P*-boronated oligonucleotides have a chirality center at the phosphorus atom and therefore are obtained as a mixture of diastereomers. Thus, the stereoregulated synthesis of *P*-boronated oligonucleotides is in progress by our group.[10c] From the hybridization studies, although the *PBX*-backbones destabilized the duplexes with complementary ODN and ORN, it was fully complemented by incorporating LNA-modified boranophosphate motifs. Further study toward the expansion of synthetically available *P*-boronated oligonucleotides and the evaluation of their physicochemical and biological properties is in progress.

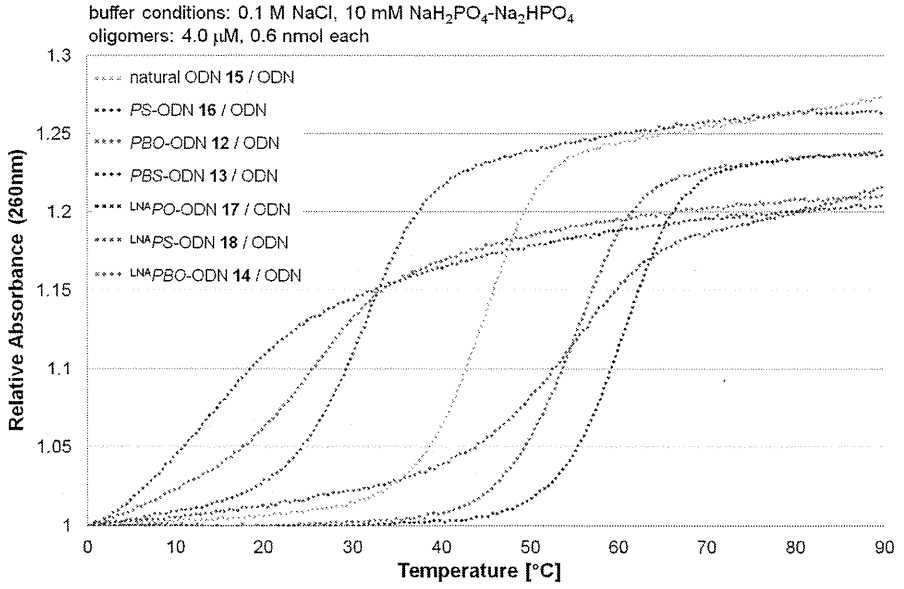

Figure 1. UV melting curves of the duplex of ODNs with complementary ODN.

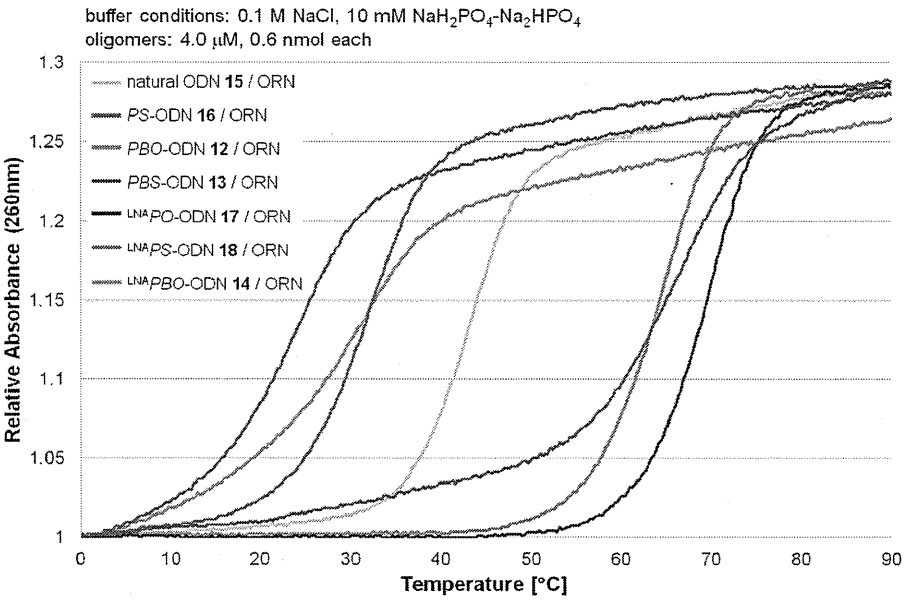

Figure 2. UV melting curves of ODNs with complementary ORN.

EXPERIMENAL SECTION

Triethylammonium 5′-*O*-Dimethoxytrityl-N^6-benzoyladenosine 3′-*H*-Boranophosphonate As a Mixture of (*Sp*)- and (*Rp*)-Diastereomers (3b). 5′-*O*-DMTr-N^6-benzoyladenosine **1b** (0.66 g, 1.0 mmol) and pyridinium *H*-boranophosphonate **2** (0.30 g, 2.0 mmol) were dried individually by repeated coevaporation with dry pyridine (3 × 3 mL for **1b** and 5 × 3 mL for **2**) and dissolved together in dry pyridine (10 mL) at 0 °C under argon. Bis(2-oxo-3-oxazolidinyl)phosphinic chloride (Bop-Cl) (0.51 g, 2.0 mmol) was added, and the mixture was stirred for 25 min at rt. The mixture was diluted with CH_2Cl_2 (50 mL) and washed with 1 M triethylammonium bicarbonate (TEAB) buffer (pH 7) (3 × 50 mL). The washings were combined and back-extracted with CH_2Cl_2 (2 × 150 mL). The organic layers were combined, dried over Na_2SO_4, filtered, and concentrated under reduced pressure. The residue was then purified by silica gel column chromatography [3.7 × 4.8 cm, 28 g of silica gel (spherical, neutral, 40–50 μm), ethyl acetate–MeOH–Et_3N (99:1:1, v/v/v) to CH_2Cl_2–MeOH–Et_3N (99.5:0.5:1–99:1:1, v/v/v)]. The fractions containing **3b** were combined and concentrated under reduced pressure. The residue was dissolved in ethyl acetate (100 mL) and washed with 1 M TEAB buffer (100 mL). The washings were combined and back-extracted with ethyl acetate (100 mL). The organic layers were combined, dried over $MgSO_4$, filtered, concentrated under reduced pressure to afford **3b** (0.61 g, 0.72 mmol, 72%) as a colorless foam. ^{1}H NMR ($CDCl_3$) δ 9.09 (br s, 1H), 8.71, 8.70 (s, s, 1H), 8.23, 8.18 (s, s, 1H), 8.04–8.00 (m, 2H), 7.63–7.58 (m, 1H), 7.54–7.49 (m, 2H), 7.42–7.38 (m, 2H), 7.31–7.16 (m, 7H), 7.31 (br d, $^1J_{PH}$ = 389 Hz, 1H), 6.81–6.76 (m, 4H), 6.61–6.55 (m, 1H), 5.13–5.02 (m, 1H), 4.49–4.42 (m, 1H), 3.77, 3.77 (s, s, 6H), 3.43, 3.42 (s, s, 2H), 3.01–2.75 (m, 9H), 1.22 (t, *J* = 7.4 Hz, 11H), 1.03–0.08 (br, 3H); ^{13}C NMR ($CDCl_3$) δ 164.7, 158.3, 158.3, 152.1, 151.4, 151.3, 149.3, 144.4, 144.3, 141.5, 141.3, 135.5, 135.4, 135.4, 133.5, 133.5, 132.6, 129.9, 129.8, 128.6, 127.9, 127.9, 127.7, 126.7, 123.4, 113.0, 112.9, 86.3, 86.2, 86.0, 85.9, 85.6, 85.6, 84.6, 84.5,

dx.doi.org/10.1021/jo500185b | J. Org. Chem. 2014, 79, 3465–3472

76.8, 76.7, 75.5, 75.5, 63.4, 63.2, 55.0, 45.1, 40.1, 39.0, 8.5; ^{31}P NMR ($CDCl_3$) δ 105.6–102.4 (m). ESI-HRMS: Calcd for $C_{38}H_{38}BN_5O_7P^-$ [M − H]$^-$ 718.2607, found 718.2615.

Triethylammonium 5′-*O*-Dimethoxytrityl-*N*^{4}-isobutyrylcytidine 3′-*H*-Boranophosphonate As a Mixture of (*Sp*)- and (*Rp*)-Diastereomers (3c). Compound **3c** was obtained in 60% (0.48 g, 0.60 mmol) from 5′-*O*-DMTr-*N*^{4}-isobutyrylcytidine **1c** (0.60 g, 1.0 mmol) and **2** (0.30 g, 2.0 mmol) as a colorless foam in a manner similar to the synthesis of **3b**, except for the reaction time (30 min) and the conditions for silica gel column chromatography [3.7 × 5.3 cm, 30 g of silica gel (spherical, neutral, 40–50 μm), ethyl acetate–MeOH–Et_3N (99:1:0.5, v/v/v) to CH_2Cl_2–MeOH–Et_3N (99:1:0.5 to 99:1:1, v/v/v)]. ^{1}H NMR ($CDCl_3$) δ 8.28, 8.26 (s, s, 1H), 8.20, 8.17 (s, s, 1H), 7.41–7.37 (m, 2H), 7.33–7.23 (m, 7H), 7.28 (br d, $^1J_{PH}$ = 394 Hz, 1H), 7.15–7.08 (m, 1H), 6.87–6.83 (m, 4H), 6.29, 6.22 (t, J = 6.0 Hz, t, J = 5.7 Hz, 1H), 5.09–5.01, 4.87–4.79 (m, m, 1H), 4.40–4.30 (m, 1H), 3.81, 3.80 (s, s, 6H), 3.46–3.44 (m, 2H), 2.95–2.87 (m, 8H), 2,57, 2.56, (sept, J = 6.9 Hz, sept, J = 6.9 Hz, 1H), 2.40–2.26 (m, 1H), 1.25–1.20 (m, 16.5H), 1.04–0.07 (br, 3H); ^{13}C NMR ($CDCl_3$) δ 177.0, 176.9, 162.3, 162.2, 158.4, 154.9, 154.9, 144.4, 144.4, 144.0, 143.9, 135.3, 135.3, 135.1, 135.1, 129.9, 129.9, 129.8, 128.0, 127.9, 127.8, 127.8, 126.9, 113.1, 113.1, 96.1, 96.0, 87.0, 86.8, 86.7, 86.6, 85.7, 85.6, 85.5, 85.4, 76.3, 76.1, 73.5, 73.4, 62.5, 62.0, 55.1, 45.2, 41.3, 40.7, 36.3, 36.2, 19.0, 18.8, 8.5; ^{31}P NMR ($CDCl_3$) δ 107.1–102.2 (m). ESI-HRMS: Calcd for $C_{34}H_{40}BN_3O_8P^-$ [M − H]$^-$ 660.2652, found 660.2653.

Triethylammonium 5′-*O*-Dimethoxytrityl-*O*^{6}-cyanoethyl-*N*^{2}-isobutyrylguanosine 3′-*H*-Boranophosphonate As a Mixture of (*Sp*)- and (*Rp*)-Diastereomers (3d). Compound **3d** was obtained in 74% (0.66 g, 0.74 mmol) from 5′-*O*-dimethoxytrityl-*O*^{6}-cyanoethyl-*N*^{2}-isobutyrylguanosine **1d** (0.67 g, 1.0 mmol) and **2** (0.30 g, 2.0 mmol) as a colorless foam in a manner similar to the synthesis of **3b**, except for the reaction time (15 min) and the conditions for silica gel column chromatography [3.7 × 4.8 cm, 28 g of silica gel (spherical, neutral, 40–50 μm), ethyl acetate–MeOH–Et_3N (99:1:1, v/v/v) to CH_2Cl_2–MeOH–Et_3N (99:1:1, v/v/v)]. ^{1}H NMR ($CDCl_3$) δ 8.01, 7.98 (s, s, 1H), 7.93, 7.90 (s, s, 1H), 7.42–7.39 (m, 2H), 7.28 (br d, $^1J_{PH}$ = 390 Hz, 1H), 7.31–7.17 (m, 7H), 6.79–6.74 (m, 4H), 6.44–6.38 (m, 1H), 5.23–5.11 (m, 1H), 4.80, 4.79 (t, J = 6.6 Hz, t, J = 6.6 Hz, 2H), 4.40–4.35 (m, 1H), 3.77, 3.77 (s, s, 6H), 3.38, 3.36 (s, s, 2H), 3.06, 3.04 (t, J = 6.6 Hz, t, J = 6.6 Hz, 2H), 3.01–2.83 (m, 9H), 2.76–2.66 (m, 2H), 1.23–1.14 (m, 18H), 1.02–0.07 (br, 3H); ^{13}C NMR ($CDCl_3$) δ 175.4, 159.4, 158.3, 152.7, 152.6, 151.5, 151.5, 144.5, 144.4, 140.8, 140.7, 135.6, 135.5, 135.5, 135.5, 129.8, 127.9, 127.7, 127.6, 126.7, 118.0, 118.0, 116.9, 112.9, 112.9, 86.2, 86.1, 85.7, 85.6, 85.4, 85.3, 84.4, 84.3, 76.1, 76.0, 75.2, 75.1, 63.4, 63.3, 61.4, 55.0, 45.2, 39.6, 38.8, 35.6, 29.5, 29.1, 19.1, 19.0, 17.9, 8.5; ^{31}P NMR ($CDCl_3$) 105.1–102.1 (m). ESI-HRMS: Calcd for $C_{38}H_{43}BN_6O_8P^-$ [M − H]$^-$ 753.2979, found 753.2986 .

Triethylammonium (1*R*,3*R*,4*R*,7*S*)-3-(*N*^{3}-Benzoylthymin-1-yl)-1-dimethoxytrityloxymethyl-2,5-dioxabicyclo[2.2.1]-heptane-7-*H*-boranophosphonate As a Mixture of (*Sp*)- and (*Rp*)-Diastereomers (3e). Compound **3e** was obtained in 75% (0.65 g, 0.75 mmol) from (1*R*,3*R*,4*R*,7*S*)-3-(*N*^{3}-benzoylthymin-1-yl)-1-dimethoxytrityloxymethyl-7-hydroxy-2,5-dioxabicyclo[2.2.1]heptanes **1e** (0.69 g, 1.0 mmol) and **2** (0.30 g, 2.0 mmol) as a colorless foam in a manner similar to the synthesis of **3b**, except for the reaction time (20 min) and the conditions for silica gel column chromatography [3.7 × 15.8 cm, 85 g of silica gel (spherical, neutral, 63-210 μm), ethyl acetate–hexane–Et_3N (67:33:0.5, v/v/v) to CH_2Cl_2–MeOH–Et_3N (99.5:0.5:0.5, v/v/v)]. ^{1}H NMR ($CDCl_3$) δ 8.00–7.93 (m, 2H), 7.83, 7.81 (d, J = 1.2 Hz, d, J = 0.9 Hz, 1H), 7.67–7.61 (m, 1H), 7.53–7.46 (m, 4H), 7.41–7.30 (m, 6H), 7.43, 7.36 (br d, $^1J_{PH}$ = 385 Hz, br d, $^1J_{PH}$ = 410 Hz, 1H), 7.24–7.21 (m, 1H), 6.89–6.85 (m, 4H), 5.63 (s, 1H), 4.92, 4.66 (d, J = 6.6 Hz, d, J = 6.6 Hz, 1H), 4.67, 4.63 (s, s, 1H), 4.00–3.72 (m, 8H), 3.57–3.44 (m, 2H), 2.90 (q, J = 7.2 Hz, 7.5H), 1.68, 1.66 (d, J = 0.9 Hz, d, J = 0.9 Hz, 3H), 1.21 (t, J = 7.2 Hz, 11H), 1.01–0.07 (br, 3H); ^{13}C NMR ($CDCl_3$) δ 168.8, 162.8, 158.5, 148.7, 148.7, 144.4, 144.2, 135.3, 135.3, 135.1, 135.0, 134.9, 134.4, 134.3, 131.3, 131.2, 130.5, 130.4, 130.0, 129.9, 129.8, 129.1, 129.1, 128.0, 128.0, 127.9, 127.8, 126.9, 113.3, 113.2, 110.3, 110.3, 88.1, 88.0, 87.9, 87.4, 86.5, 78.6, 78.5, 74.6, 74.4, 72.2, 72.1, 71.5, 57.8, 57.5, 55.1, 45.3, 12.6, 12.5, 8.4; ^{31}P NMR ($CDCl_3$) δ 107.5 (m). ESI-HRMS: Calcd for $C_{39}H_{39}BN_2O_{10}P^-$ [M − H]$^-$ 737.2441, found 737.2443.

A General Procedure for the Manual Solid-Phase Synthesis of *PBH*-ODN 2mers (for the synthesis of *PBO*- and *PBS*-ODN 2mers). CPG loaded with 5′-*O*-DMTr-*N*^{3}-benzoylthymidine *via* a succinate linker (0.5 μmol) was treated with 3% dichloroacetic acid (DCA) in dry CH_2Cl_2 (4 × 15 s), washed with dry CH_2Cl_2 and CH_3CN, and then dried *in vacuo* for 10 min. Condensation reaction of the corresponding 2′-deoxyribonucleoside 3′-*H*-boranophosphonate monomer units **3a–d** (0.1 M) was carried out in the presence of 1,3-dimethyl-2-(3-nitro-1,2,4-triazol-1-yl)-2-pyrrolidin-1-yl-1,3,2-diazaphospholidinium hexafluorophosphate (MNTP) (0.25 M) and 2,6-lutidine (0.6 M) in dry CH_3CN for 1 min under argon. The solid support was then washed with dry CH_3CN and CH_2Cl_2. The 5′-*O*-DMTr group of the resultant *PBH*-ODN 2mer was removed by treatment with 3% DCA in CH_2Cl_2–Et_3SiH (1:1,v/v) (6 × 5 s), and the solid support was washed with dry CH_2Cl_2 and CH_3CN and dried *in vacuo* for 10 min. The resultant *PBH*-ODN 2mer was oxidized or sulfurized as described below.

Synthesis of *PBO*-ODN 2mers (6a–d) (Table 2, entries 1–4). *PBH*-ODN 2mer generated on the CPG as above was oxidized with *i*-Pr_2NEt (0.3 M), CCl_4 (1 M) and H_2O (0.5 M) in dry CH_3CN at rt for 30 min under argon, and the CPG was successively washed with dry CH_3CN and CH_2Cl_2. The CPG was then treated with 25% NH_3 aq–EtOH (3:1, v/v) at 30 °C for 3 h (for $T_{PBO}T$ **6a**), at 30 °C for 12 h (for $A_{PBO}T$ **6b** and $C_{PBO}T$ **6c**), or at 50 °C for 12 h (for $G_{PBO}T$ **6d**), filtered, and washed with EtOH (4 mL). The filtrate and washings were combined and concentrated to dryness under reduced pressure, and the residue was analyzed by RP-HPLC and MALDI-TOF MS. RP-HPLC was performed with a linear gradient of 0–30% CH_3CN in 0.1 M triethylammonium acetate (TEAA) buffer (pH 7) for 60 min at 30 °C at a flow rate of 0.5 mL/min using a column of C_{18}. MALDI-TOF MS: Calcd for $T_{PBO}T$ (**6a**) [M − H]$^-$ 543.17, found 543.51. Calcd for $dA_{PBO}T$ (**6b**) [M − H]$^-$ 552.18, found 552.21. Calcd for $dC_{PBO}T$ (**6c**) [M − H]$^-$ 528.17, found 528.10. Calcd for $dG_{PBO}T$ (**6d**) [M − H]$^-$ 568.17, found 568.10.

Synthesis of *PBS*-ODN 2mers (7a–d) (Table 2, entries 5–8). *PBH*-ODN 2mer generated on CPG as above was sulfurized with *i*-Pr_2NEt (1 M) and dimethylthiuram disulfide (DTD) (0.3 M) in dry CH_3CN at rt for 1 h under argon, and the CPG was successively washed with dry CH_3CN and CH_2Cl_2. The CPG was then treated with 25% NH_3 aq at 30 °C for 3 h (for $T_{PBS}T$ **7a**), at 30 °C for 12 h (for $A_{PBO}T$ **7b** and $C_{PBO}T$ **7c**), or at 50 °C for 12 h (for $G_{PBO}T$ **7d**), filtered, and washed with EtOH (1 mL). The filtrate and washings were combined and concentrated to dryness under reduced pressure, and the residue was analyzed by RP-HPLC and MALDI-TOF MS. RP-HPLC was performed with a linear gradient of 0–30% CH_3CN in 0.1 M TEAA buffer (pH 7) for 60 min at 30 °C at a flow rate of 0.5 mL/min using a column of C_{18}. MALDI-TOF MS: Calcd for $T_{PBS}T$ (**7a**) [M − H]$^-$ 559.14, found 559.45. Calcd for $dA_{PBS}T$ (**7b**) [M − H]$^-$ 568.16, found 568.68. Calcd for $dC_{PBS}T$ (**7c**) [M − H]$^-$ 544.14, found 544.09. Calcd for $dG_{PBS}T$ (**7d**) [M − H]$^-$ 584.15, found 584.53.

Synthesis of $T_{PBN}T$ (8) (Table 2, entry 10). 5′-*O*-DMTr-$T_{PBH}T$ (Scheme 2, **5**, n = 0) was synthesized on the CPG as described above. The $T_{PBH}T$ was treated with CCl_4 (1 M) and 4-(2-aminoethyl)-morpholine (0.5 M) in dry CH_3CN at rt for 30 min under argon, and the CPG was then successively washed with dry CH_3CN and CH_2Cl_2. The 5′-*O*-DMTr group was removed by treatment with 3% DCA in CH_2Cl_2–Et_3SiH (1:1, v/v) (6 × 5 s), and the CPG was washed with dry CH_2Cl_2. The CPG was then treated with 25% NH_3 aq–EtOH (3:1, v/v) at 30 °C for 1 h, filtered, and washed with EtOH (4 × 1 mL). The filtrate and washings were combined and concentrated to dryness under reduced pressure, and the residue was analyzed by RP-HPLC and MALDI-TOF MS. RP-HPLC was performed with a linear gradient of 0–45% CH_3CN in 0.1 M TEAA buffer (pH 7) for 60 min at 30 °C at a flow rate of 0.5 mL/min using a column of C_{18}. MALDI-TOF MS: Calcd for $[M + H]^+$ 657.28, found 657.31.

dx.doi.org/10.1021/jo500185b | J. Org. Chem. 2014, 79, 3465–3472

Synthesis of 2′-Deoxy *PBO* and *PBS*-ODN 12mers. CPG loaded with 5′-*O*-DMTr-N^3-benzoylthymidine or 5′-*O*-DMTr-N^4-isobutyrylcytidine (0.5 μmol) *via* a succinate linker was treated with 3% DCA in dry CH_2Cl_2 (4 × 15 s), washed with dry CH_2Cl_2 and CH_3CN, and dried *in vacuo* for 10 min. Chain elongation was performed by repeating 11 times the following steps (a) and (b). (a) Condensation of the corresponding nucleoside 3′-*H*-boranophosphonate monomer units **3a**–**d** (0.1 M) in the presence of MNTP (0.25 M) and 2,6-lutidine (0.6 M) in dry CH_3CN for 1 min under argon and subsequent washing with dry CH_3CN and CH_2Cl_2. (b) Removal of 5′-*O*-DMTr group by treatment with 3% DCA in CH_2Cl_2–Et_3SiH (1:1, v/v) (6 × 5 s), subsequent washing with dry CH_2Cl_2 and CH_3CN, and drying *in vacuo* for 5 min. The resultant *PBH*-ODN 12mers were oxidized or sulfurized as described above. After the conversions, the CPG was treated with 25% NH_3 aq–EtOH (3:1, v/v) at 30 °C for 12 h (for $T(_{PBO}T)_{11}$ (**9**)), 25% NH_3 aq at 30 °C for 12 h (for $T(_{PBS}T)_{11}$ (**10**)), 25% NH_3 aq–EtOH (3:1, v/v) at 50 °C for 12 h (for *PBO*-ODN 12mer (5′-GCA TTG GTA TTC-3′) (**12**)) and 25% NH_3 aq at 50 °C for 12 h (for *PBS*-ODN 12mer (5′-GCA TTG GTA TTC-3′) (**13**)). Then, the CPG was filtered and washed with EtOH (4 × 1 mL). The filtrate and washings were combined and concentrated to dryness under reduced pressure. The residue was dissolved in H_2O (4 mL) and washed with $CHCl_3$ (6 × 500 μL). The aqueous layer was analyzed by RP-HPLC and MALDI-TOF MS. RP-HPLC analysis was performed with a linear gradient of 0–60% CH_3CN in 0.1 M TEAA buffer (pH 7) for 60 min at 30 °C at a flow rate of 0.5 mL/min using a column of C_{18}. Purification by RP-HPLC was performed with a linear gradient of 8–44% CH_3CN in 0.1 M TEAA buffer (pH 7) for 90 min at rt at a flow rate of 1 mL/min using a column of C_{18}. Isolated yields: 28% ($T(_{PBO}T)_{11}$ (**9**)); 31% ($T(_{PBS}T)_{11}$ (**10**)); 44% (*PBO*-ODN 12mer (5′-GCA TTG GTA TTC-3′) (**12**)); 16% (*PBS*-ODN 12mer (5′-GCA TTG GTA TTC-3′) (**13**)). MALDI-TOF MS: Calcd for $T(_{PBO}T)_{11}$ (**9**) $[M - H]^-$ 3564.01, found 3564.17; Calcd for $T(_{PBS}T)_{11}$ (**10**) $[M - H]^-$ 3739.75, found 3739.05; Calcd for *PBO*-ODN 12mer (5′-GCA TTG GTA TTC-3′) (**12**) $[M - H]^-$ 3627.05, found 3626.82; Calcd for *PBS*-ODN 12mer (5′-GCA TTG GTA TTC-3′) (**13**) $[M - H]^-$ 3802.80, found 3801.52.

Synthesis of ^{LNA}*PBO*-ODN 12mer (5′-GCA T^LT^LG GT^LA T^LT^LC-3′) (14). ^{LNA}*PBH*-ODN 12mer (5′-GCA $\mathbf{T^LT^L}$G GT^LA T^LT^LC-3′) synthesized on CPG as above was oxidized[25] with Et_3N (0.1 M) in CCl_4–2,6-lutidine–H_2O (5:12.5:1, v/v/v) at rt for 1 h under argon, and the CPG was successively washed with dry CH_3CN and CH_2Cl_2. The CPG was then treated with 25% NH_3 aq–EtOH (3:1, v/v) at 50 °C for 12 h, filtered, and washed with EtOH (4 × 1 mL). The filtrate and washings were combined and concentrated to dryness under reduced pressure. The residue was dissolved in H_2O (4 mL) and washed with $CHCl_3$ (6 × 500 μL). The aqueous layer was then analyzed by RP-HPLC, ion-exchange HPLC (IE-HPLC) and MALDI-TOF MS. RP-HPLC analysis was performed with a linear gradient of 0–60% CH_3CN in 0.1 M TEAA buffer (pH 7) for 60 min at 30 °C at a flow rate of 0.5 mL/min using a column of C_{18}. IE-HPLC analysis and purification were performed with a linear gradient of 0–1 M NaCl, 50–25% CH_3CN in 10 mM Tris–HCl buffer (pH 8) for 20 min at rt at a flow rate of 0.8 mL/min using a column of quaternary ammonium anion exchange resin. Fractions containing **14** (see Supporting Information, page S10, *Figure S9* (b), fraction D) were combined and concentrated to dryness under reduced pressure and desalted with a short cartridge of C_{18}. The cartridge was washed with H_2O (6 × 5 mL), and then the desired product was eluted with 50% CH_3CN. Isolated yield: 7%. MALDI-TOF MS: Calcd for $[M - H]^-$ 3767.02, found 3767.06.

$T(_{PBN}T)_{11}$ (11). 5′-*O*-DMTr-$T(_{PBH}T)_{11}$ (Scheme 2, **5**, n = 10) synthesized by repeating condensation and detritylation was aminated as well as $T_{PBN}T$ **8**. The 5′-*O*-DMTr group was removed by treatment with 3% DCA in CH_2Cl_2–Et_3SiH (1:1, v/v) (6 × 5 s) and washed with dry CH_2Cl_2. The CPG was treated with 25% NH_3 aq–EtOH (3:1, v/v) at 30 °C for 1 h, filtered, and washed with EtOH (4 × 1 mL). The filtrate and washings were combined and concentrated to dryness under reduced pressure. The residue was then analyzed by RP-HPLC and MALDI-TOF MS. RP-HPLC analysis and purification were performed with a linear gradient of 0–60% CH_3CN in 0.1 M TEAA buffer (pH 7) for 60 min at 30 °C at a flow rate of 0.5 mL/min using a column of C_{18}. Isolated yield: 10%. MALDI-TOF MS: Calcd for $[M + H]^+$ 4799.12, found 4799.43.

Thermal Denaturation Studies (for natural, *PS*, *PBO*, *PBS*, ^{LNA}*PO*, ^{LNA} *PS*, and ^{LNA}*PBO*-ODN). Pairs of complementary strands (1:1 molar ratio, 4.0 μM, 0.6 nmol each) were dissolved in 10 mM NaH_2PO_4–Na_2HPO_4 buffer solutions (pH 7.0) containing 0.1 or 1 M NaCl. The solutions were heated for 10 min at 90 °C or for 15 min at 95 °C and cooled to 0 °C at a rate of −0.5 °C/min, and then left at 0 °C for 1 h. Denaturation studies were carried out in a 1 cm path length quartz cell. UV absorbance values (260 nm) were recorded at a rate of 0.5 °C/min from 0 to 90 °C or 100 °C.

Thermal Denaturation Studies (for *PBN*-ODN). Pairs of complementary strands (1:1 molar ratio, 4.0 μM, 0.6 nmol each) were dissolved in (a) 10 mM NaH_2PO_4–Na_2HPO_4 buffer solutions (pH 7.0) containing 0, 0.1, or 1 M NaCl, (b) 10 mM NaH_2PO_4–Na_2HPO_4 (pH 5.8) without NaCl or (c) 10 mM NaH_2PO_4 (pH 5.0) without NaCl. The solutions were heated for 10 min at 90 °C and cooled to 0 °C at a rate of −0.5 °C/min, and then left at 0 °C for 1 h. Denaturation studies were carried out in a 1 cm path length quartz cell. UV absorbance values (260 nm) were recorded at a rate of 0.5 °C/min from 0 to 90 °C.

■ ASSOCIATED CONTENT

Supporting Information

^1H, ^{13}C, and ^{31}P NMR spectra, HPLC profiles, and UV melting curves. This material is available free of charge via the Internet at http://pubs.acs.org.

■ AUTHOR INFORMATION

Corresponding Author

*E-mail: twada@rs.tus.ac.jp

Notes

The authors declare no competing financial interest.

■ ACKNOWLEDGMENTS

We thank Prof. Dr. Satoshi Obika (Osaka University) for kindly providing LNA thymidine. This work was supported by JST, CREST.

■ REFERENCES

(1) (a) Kurreck, J. *Eur. J. Biochem.* **2003**, *270*, 1628–1644. (b) Wilson, C.; Keefe, A. D. *Curr. Opin. Chem. Biol.* **2006**, *10*, 607–614. (c) Yano, J.; Smyth, G. E. *Adv. Polym. Sci.* **2012**, *249*, 1–48.

(2) Debart, F.; Abes, S.; Deglane, G.; Moulton, H. M.; Clair, P. M.; Gait, J.; Vasseur, J.-J.; Lebleu, B. *Curr. Top. Med. Chem.* **2007**, *7*, 727–737.

(3) (a) Sands, H.; Gorey-Feret, L. J.; Cocuzza, A. J.; Hobbs, F. W.; Chidester, D.; Trainor, G. L. *Mol. Pharmacol.* **1994**, *45*, 932–943. (b) Henry, S. P.; Giclas, P. C.; Leeds, J.; Pangburn, M.; Auletta, C.; Levin, A. A.; Kornbrust, D. J. *J. Pharmacol. Exp. Ther.* **1997**, *281*, 810–816. (c) Levin, A. A. *Biochim. Biophys. Acta* **1999**, *1489*, 69–84. (d) Zon, G. *New J. Chem.* **2010**, *34*, 795–804.

(4) Jiang, K. *Nat. Med.* **2013**, *19*, 252.

(5) (a) Hall, I. H.; Burnham, B. S.; Rajendran, K. G.; Chen, S. Y.; Sood, A.; Spielvogel, B. F.; Shaw, B. R. *Biomed Pharm.* **1993**, *47*, 79–87. (b) Hall, A. H. S.; Wan, J.; Shaughnessy, E. E.; Shaw, B. R.; Alexander, K. A. *Nucleic Acids Res.* **2004**, *32*, 5991–6000.

(6) (a) Lesnikowski, Z. J.; Schinazi, R. F. *J. Org. Chem.* **1993**, *58*, 6531–6534. (b) Summers, J. S.; Shaw, B. R. *Curr. Med. Chem.* **2001**, *8*, 1147–1155. (c) Lesnikowski, Z. J. *Eur. J. Org. Chem.* **2003**, *23*, 4489–4500. (d) Li, P.; Sergueeva, Z. A.; Dobrikov, M.; Shaw, B. R. *Chem. Rev.* **2007**, *107*, 4746–4796. (e) Martin, A. R.; Vasseur, J.-J.; Smietana, M. *Chem. Soc. Rev.* **2013**, *42*, 5684–5713. (f) Kwiatkowska, A.; Sobczak, M.; Mikolajczyk, B.; Janczak, S.; Olejniczak, A. B.; Sochacki,

M.; Lesnikowski, Z. J.; Nawrot, B. *Bioconjugate Chem.* **2013**, *24*, 1017–1026.
(7) (a) Sood, A.; Shaw, B. R.; Spielvogel, B. F. *J. Am. Chem. Soc.* **1990**, *112*, 9000–9001. (b) Sergueev, D.; Hasan, A.; Ramaswamy, M.; Shaw, B. R. *Nucleosides Nucleotides* **1997**, *16*, 1533–1538. (c) Sergueev, D. S.; Shaw, B. R. *J. Am. Chem. Soc.* **1998**, *120*, 9417–9427. (d) Lin, J.; Shaw, B. R. *Chem. Commun.* **1999**, 1517–1518. (e) Lin, J.; Shaw, B. R. *Nucleosides, Nucleotides Nucleic Acids* **2001**, *20*, 587–596. (f) Sergueev, D. S.; Sergueeva, Z. A.; Shaw, B. R. *Nucleosides, Nucleotides Nucleic Acids* **2001**, *20*, 789–795.
(8) Zhang, J.; Terhorst, T.; Matteucci, M. D. *Tetrahedron Lett.* **1997**, *38*, 4957–4960.
(9) (a) Higson, A. P.; Sierzchala, A.; Brummel, H.; Zhao, Z.; Caruthers, M. H. *Tetrahedron Lett.* **1998**, *39*, 3899–3902. (b) Brummel, H. A.; Caruthers, M. H. *Tetrahedron Lett.* **2002**, *43*, 749–751. (c) McCuen, H. B.; Noé, M. S.; Sierzchala, A. B.; Higson, A. P.; Caruthers, M. H. *J. Am. Chem. Soc.* **2006**, *128*, 8138–8139. (d) McCuen, H. B.; Noé, M. S.; Olesiak, M.; Sierzchala, A. B.; Caruthers, M. H.; Higson, A. P. *Phosphorus, Sulfur Silicon Relat. Elem.* **2008**, *183*, 349–363. (e) Olesiak, M.; Krivenko, A.; Krishna, H.; Caruthers, M. H. *Phosphorus, Sulfur Silicon Relat. Elem.* **2011**, *186*, 921–932. (f) Krishna, H.; Caruthers, M. H. *J. Am. Chem. Soc.* **2011**, *133*, 9844–9854. (g) Roy, S.; Olesiak, M.; Shang, S.; Caruthers, M. H. *J. Am. Chem. Soc.* **2013**, *135*, 6234–6241.
(10) (a) Shimizu, M.; Wada, T.; Oka, N.; Saigo, K. *J. Org. Chem.* **2004**, *69*, 5261–5268. (b) Shimizu, M.; Saigo, K.; Wada, T. *J. Org. Chem.* **2006**, *71*, 4262–4269. (c) Iwamoto, N.; Oka, N.; Wada, T. *Tetrahedron Lett.* **2012**, *53*, 4361–4364.
(11) Kraszewski, A.; Stawinski, J. *Pure Appl. Chem.* **2007**, *79*, 2217–2227.
(12) Belabassi, Y.; Antczak, M. I.; Tellez, J.; Montchamp, J.-L. *Tetrahedron* **2008**, *64*, 9181–9190.
(13) (a) Higashida, R.; Oka, N.; Kawanaka, T.; Wada, T. *Chem. Commun.* **2009**, 2466–2468. (b) Oka, N.; Takayama, Y.; Ando, K.; Wada, T. *Bioorg. Med. Chem. Lett.* **2012**, *22*, 4571–4574.
(14) Grabulosa, A.; Granell, J.; Muller, G. *Coord. Chem. Rev.* **2007**, *251*, 25–90.
(15) (a) Obika, S.; Nanbu, D.; Hari, Y.; Morio, K.; In, Y.; Ishida, T.; Imanishi, T. *Tetrahedron Lett.* **1997**, *38*, 8735–8738. (b) Singh, S. K.; Nielsen, P.; Koshkin, A. A.; Wengel, J. *Chem. Commun.* **1998**, 455–456. (c) Koshkin, A. A.; Singh, S. K.; Nielsen, P.; Rajwanshi, V. K.; Kumar, R.; Meldgaard, M.; Olsen, C. E.; Wengel, J. *Tetrahedron* **1998**, *54*, 3607–3630. (d) Obika, S.; Rahman, S. M. A.; Fujisaka, A.; Kawada, Y.; Baba, T.; Imanishi, T. *Heterocycles* **2010**, *81*, 1347–1392.
(16) We have reported the solution-phase synthesis of boranophosphorothioate nucleoside and dinucleoside derivatives *via* the *H*-boranophosphonate precursors. See, ref 13.
(17) Synthesis of dithymidine boranophosphorothioate via boranophosphotriester has also been reported. See refs 7d and 7e.
(18) *P*-(2-Morpholinoethylamino) substituent has been used to develop polycationic phosphoramidate oligonucleotides. Letsinger, R. L.; Singman, C. N.; Histand, G.; Salunkhe, M. *J. Am. Chem. Soc.* **1988**, *110*, 4470–4471.
(19) Oka, N.; Shimizu, M.; Saigo, K.; Wada, T. *Tetrahedron* **2006**, *62*, 3667–3673.
(20) (a) Sergueeva, Z. A.; Sergueev, D. S.; Shaw, B. R. *Nucleosides, Nucleotides Nucleic Acids* **2001**, *20*, 941–945. (b) Shimizu, M.; Tamura, K.; Wada, T.; Saigo, K. *Tetrahedron Lett.* **2004**, *45*, 371–374.
(21) (a) Froehler, B. C. *Tetrahedron Lett.* **1986**, *27*, 5575–5578. (b) Tömösközi, I.; Gács-Baitz, E.; Ötvös, L. *Tetrahedron* **1995**, *51*, 6797–6804.
(22) Song, Q.; Wang, Z.; Sanghvi, Y. S. *Nucleosides, Nucleotides Nucleic Acids* **2003**, *22*, 629–633.
(23) See the SI.
(24) Straarup, E. M.; Fisker, N.; Hedtjärn, M.; Lindholm, M. W.; Rosenbohm, C.; Aarup, V.; Hansen, H. F.; Ørum, H.; Hansen, J. B. R.; Koch, T. *Nucleic Acids Res.* **2010**, *38*, 7100–7111.
(25) ^{LNA}*PBO*-ODN **14** was synthesized by using oxidation conditions which were different from those for 2′-deoxy *PBO*-ODNs. Maier, M. A.; Guzaev, A. P.; Manoharan, M. *Org. Lett.* **2000**, *2*, 1819–1822.
(26) It has also been reported that methylboranophosphonate-ODNs have higher affinity to complementary ORNs than ODNs. See, ref 9f.

Tetrahedron Letters 55 (2014) 1991–1993

Contents lists available at ScienceDirect

Tetrahedron Letters

journal homepage: www.elsevier.com/locate/tetlet

3-Nitro-1,2,4-triazol-1-yl-tris(pyrrolidin-1-yl)phosphonium hexafluorophosphate (PyNTP) as a condensing reagent for solid-phase peptide synthesis

Keita Saito [a], Takeshi Wada [a,b,*]

[a] Department of Medical Genome Sciences, Graduate School of Frontier Sciences, The University of Tokyo, Bioscience Building 702, 5-1-5 Kashiwanoha, Kashiwa, Chiba 277-8562, Japan
[b] Faculty of Pharmaceutical Sciences, Tokyo University of Science, 2641 Yamazaki, Noda, Chiba 278-8510, Japan

ARTICLE INFO

Article history:
Received 13 January 2014
Revised 5 February 2014
Accepted 7 February 2014
Available online 15 February 2014

Keywords:
Solid-phase peptide synthesis
Condensing reagent
Aminoisobutyric acid
Racemization

ABSTRACT

Solid-phase oligopeptide synthesis has been well developed and most short oligopeptides can now be easily synthesized. However, when a desired oligopeptide forms a secondary structure or includes less reactive amino acids such as aminoisobutyric acid, its terminal amino groups become less reactive and synthesis of the desired oligopeptides becomes difficult. To expand the number of synthetic peptide sequences, we have developed efficient coupling conditions using 3-nitro-1,2,4-triazol-1-yl-tris (pyrrolidin-1-yl)phosphonium hexafluorophosphate (PyNTP) as a highly reactive condensing reagent on an unswellable solid support. PyNTP demonstrated higher reactivity than conventional condensing reagents and the optical purity of the synthesized oligopeptides was sufficiently high for application to general oligopeptide synthesis.

Condensing reagents for solid-phase peptide synthesis (SPPS) such as HBTU,[1] HATU,[2] PyBOP,[3] PyAOP,[4] and COMU[5] (Fig. 1) have been extensively developed and diverse sequences of oligopeptides can now be synthesized. However, longer peptide chains may fold into secondary structures, with consequent reduction in the reactivity of their terminal amino groups and the synthesis of long oligopeptides is largely precluded. Oligopeptides containing a high portion of less reactive amino acids such as aminoisobutyric acid (Aib) are similarly affected.

To synthesize such oligopeptides, solid-phase synthesis is sometimes replaced with stepwise solution-phase syntheses via aziridine/oxazolone intermediates or using building blocks.[6,7] As in standard solution-phase synthesis, the tedious process of isolation is necessary for each step. Solid-phase synthesis is very advantageous in purification, since removal of excess reagents and byproducts is possible by washing, therefore, more efficient methodologies for synthesizing oligopeptides on solid supports are still required.

Especially, when amino acids are coupled with less reactive terminal amino groups, common peptide coupling reagents such as HBTU, HATU, PyBOP, or PyAOP yield acylated benzotriazole and/or azabenzotriazole as a reactive intermediate whether they are guanidinium/uronium type reagents or phosphonium type reagents.[3,4] These intermediates exist in equilibrium between the stable *N*-form and the reactive *O*-form.[8] The formation of less reactive intermediates, which would reduce the overall reactivity, is preventable by two strategies (Scheme 1). The first strategy inhibits formation of the *N*-form, while the second increases the ability of the leaving group to depart the *N*-form. COMU employs the former strategy, in which the leaving group is ethyl (hydroxyimino)cyanoacetate, permits only the *O*-form as a highly reactive intermediate.[5]

In this study, we focused on the latter strategy; activating the *N*-form by introducing an electron withdrawing group to the leaving group. Previously, we synthesized a guanidium-type

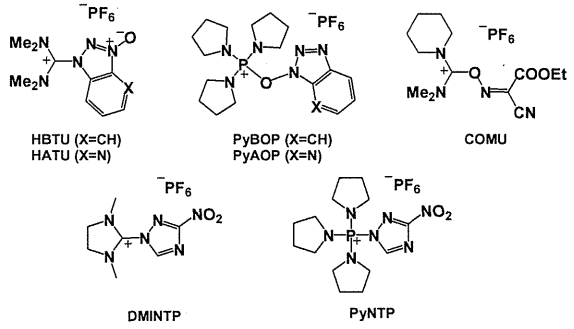

Figure 1. The structure of HBTU, HATU, PyBOP, PyAOP, COMU, DMINTP, and PyNTP.

* Corresponding author. Tel./fax: +81 4 7121 3671.
E-mail address: twada@rs.tus.ac.jp (T. Wada).

http://dx.doi.org/10.1016/j.tetlet.2014.02.013
0040-4039/

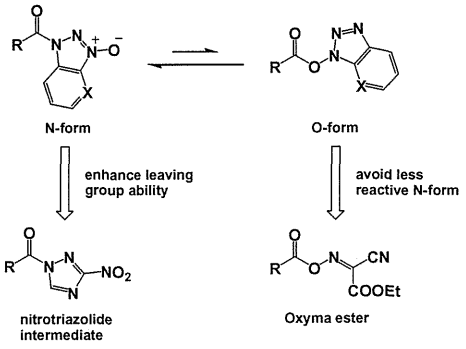

Scheme 1. Reactive intermediates generated by HBTU, HATU, PyBOP, PyAOP, COMU, and PyNTP.

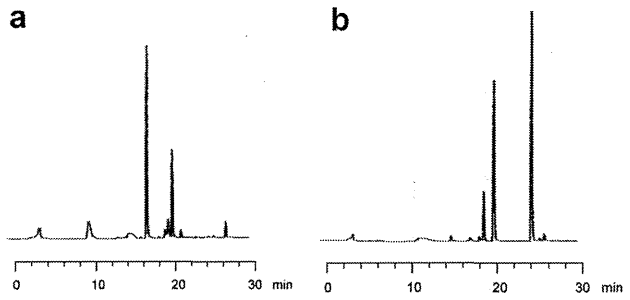

Figure 2. HPLC profiles of crude H-(Aib)$_4$-Tyr-NH$_2$. (a) Conditions: *N*-Fmoc amino acid (5 equiv), COMU (7.5 equiv), DIPEA (10 equiv)/NMP; (b) Conditions: *N*-Fmoc amino acid (5 equiv), PyNTP (7.5 equiv), DIPEA (10 equiv)/NMP.

condensing reagent for esterification, namely, 3-nitro-1,2,4-triazole as a leaving group1-(1′,3′-dimethyl-1*H*-imidazol-2′-yl)-3-nitro-1,2,4-triazol hexafluorophosphate (DMINTP, Fig. 1), whose leaving group was 3-nitro-1,2,4-triazol. However, DMINP immediately reacted with alcohol in the presence of 2,6-lutidine, and proved ineffective for esterification.[9] Thus, we designed a phosphonium-type condensing reagent, 3-nitro-l,2,4-triazol-l-yl-tris (pyrrolidin-1-yl)phosphonium hexafluorophosphate (PyNTP, Fig. 1), which facilitates the synthesis of phosphate, phosphonate, and carboxylic acid ester derivatives.[10–12] Here, we report an efficient method for solid-phase oligopeptide synthesis using PyNTP.

The capability of PyNTP as a peptide coupling reagent was evaluated on a synthetic pentapeptide target, H-(Aib)$_4$-Tyr-NH$_2$. As mentioned above, Aib is one of the least reactive amino acids due to its sterically hindered amino and carboxyl groups. In addition, the 3_{10}-helical structure of oligo-Aib obscures the terminal amino group and markedly disrupts condensation.[13,14] For concise HPLC analysis of the resultant peptides, l-tyrosine was incorporated as a UV marker.

First, we compared PyNTP with COMU under standard solid-phase peptide coupling conditions (Fig. 2). We applied the Rink amide NH-SAL-PEG resin (TentaGel S RAM, loading amount: 230 μmol/g), in which polyethylene glycol is inserted between Rink amide and the resin, rendering the compound sterically less hindered and suitable for synthesizing oligopeptides bearing less reactive amino acids. Under COMU coupling, the major product was the dipeptide H-Aib-Tyr-NH$_2$, and the longest peptide detectable by MALDI-TOF-MS was the trimer H-(Aib)$_2$-Tyr-NH$_2$ (Fig. 2a). On the other hand, under PyNTP, the desired H-(Aib)$_4$-Tyr-NH$_2$ was obtained as the major product in 49% yield (Fig. 2b). Notably, effective H-(Aib)$_4$-Tyr-NH$_2$ synthesis was achieved merely by replacing COMU by PyNTP.

Conventional solvents for SPPS are *N*-methylpyrrolidone (NMP) and *N,N*-dimethylformamide (DMF). In these solvents, the resin swells up and enhances the coupling efficiency. However, while PyNTP increased the reactivity during H-(Aib)$_4$-Tyr-NH$_2$ synthesis, NMP was not necessarily the best solvent for the coupling. However, from the viewpoint of solvent optimization, swellable resins limit the choice of solvents to those that swell the resins. Unswellable resins impose no such restrictions and accommodate wider range of solvents.

Unswellable resins are broadly used in solid-phase nucleic acid synthesis, where they yield 100mers and higher.[15] Generally, reproducible oligonucleotide synthesis is achieved by 20 equiv of monomer per coupling.[16] Thus, we followed a standard protocol for oligonucleotide synthesis using 20 equiv of monomer. For a fair comparison, we also synthesized the objective pentapeptide using HATU, COMU, and PyNTP with 20 equiv of monomer on a swellable solid support (Table 1, entries 1–3). However, because the concentration of monomer was retained constant, and is the more important quantity, similar results were obtained using 5 equiv of monomer (Fig. 2).

As an unswellable resin, Rink amide-introduced (loading amount: 68.2 μmol/g) highly-crosslinked polystyrene (Custom Primer Support®,GE Healthcare) was employed in this study. To

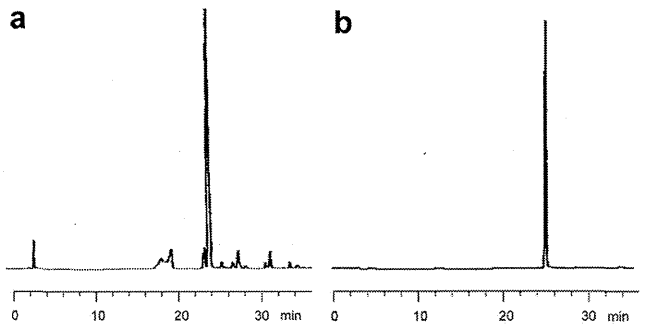

Figure 3. (a) HPLC profile of crude H-(Aib)$_4$-Tyr-NH$_2$ (Table 1, entry 6); (b) HPLC profile of purified H-(Aib)$_4$-Tyr-NH$_2$.

Table 1
Synthesis of H-(Aib)$_n$-Tyr-NH$_2$ using different coupling reagents and solvents

Entry	Resin	Condensing reagent	Solvent	2mer (%)	3mer (%)	4mer (%)	5mer (%)	Byproducts
1	Rink amide NH-SAL-PEG	COMU	NMP	32	10	n.d.	0	58
2	Rink amide NH-SAL-PEG	HATU	NMP	56	14	4	n.d.	26
3	Rink amide NH-SAL-PEG	PyNTP	NMP	0	19	39	42	0
4	CPS	PyNTP	Pyridine	0	7	20	58	15
5	CPS	PyNTP	MeCN	0	13	34	53	0
6	CPS	PyNTP	NMP	0	7	9	64	21

Conditions: *N*-Fmoc amino acid (20 equiv), condensing reagent (80 equiv), DIPEA (80 equiv) for 15 min.
Yields were calculated on the basis of peak area of the HPLC profiles detected at 280 nm.[17]

Table 2
Synthesis of Z-Phg-Pro-NH_2 on solid support and the observation of diastereomers

Entry	Resin	Condensing reagent	Monomer (equiv)	Solvent	d.r. (%)
1	Rink amide NH-SAL-PEG	HATU	5	NMP	92
2	Rink amide NH-SAL-PEG	PyNTP	5	NMP	94
3[a]	CPS	PyNTP	20	MeCN	96
4[b]	CPS	PyNTP	20	NMP	96

Diastereomer ratios were calculated on the basis of peak area of the HPLC profiles detected at 200 nm.[18]
[a] The conditions for entry 5 in Table 1 were employed.
[b] The conditions for entry 6 in Table 1 were employed.

dissolve the *N*-Fmoc amino acids, pyridine, acetonitrile, and NMP were chosen as solvents (Table 1, entries 4–6). According to the results of Table 1, PyNTP, unlike HATU and COMU, afforded H-$(Aib)_4$-Tyr-NH_2 under all tested conditions. Among the above-mentioned solvents, acetonitrile suppressed the side reactions and yielded simpler profiles, but afforded lower coupling efficiency than pyridine and NMP. Comparing NMP with pyridine, suppression of side reactions and coupling efficiency were higher in NMP than in pyridine. Notably, coupling efficiency was improved on the unswellable resin relative to the swellable resin. Condensation on a swellable resin is usually more efficient because the conditions in swelled resin approach those of homogeneous solution-phase reactions.

Isolation of H-$(Aib)_4$-Tyr-NH_2 was attempted from the crude sample of entry 6 in Table 1 (Fig. 3). A pure product was obtained with 14% yield in a single purification by reversed-phase HPLC (RP-HPLC). Compared with the crude yield, the isolated yield was low as a consequence of the loss during the purification.

Before extending this methodology to the synthesis of natural amino acids, it must be clarified that PyNTP affords optically pure oligopeptides without racemization.

The degree of racemization was measured by condensing *N*-benzyloxycarbonyl-protected phenylglycine (Z-Phg-OH) with L-proline on a solid support. Phenylglycine is notoriously susceptible to racemizaton and optically pure oligopeptides are difficult to obtain. Optically pure oligomers of proline are rendered similarly elusive by the less reactive secondary amino group. The ratio of (L, L) and (D, L) diastereomers of Z-Phg-Pro-NH_2 was determined by RP-HPLC (Table 2).

Under conditions of standard SPPS, the diastereomeric ratio of Z-Phg-Pro-NH_2 synthesized with PyNTP was comparable to that of Z-Phg-Pro-NH_2 synthesized with HATU conditions for the standard solid-phase peptide synthesis (entries 1 and 2 in Table 2). Moreover, unswellable resin yielded slightly better results than standard swellable resin.

In conclusion, we developed efficient coupling conditions for oligopeptide synthesis using PyNTP and unswellable resin. PyNTP was highly reactive and applicable to conventional solid-phase synthesis of oligopeptides containing less reactive amino acids. The use of an unswellable resin also enhanced the coupling efficiency and enabled oligopeptide synthesis in a wider range of solvents. Although racemization of activated monomers is of primary concern when developing novel condensing reagents, PyNTP inhibited epimerization at least as effectively as HATU. We expect that the present method is suitable for synthesizing long oligopeptides or those containing less reactive amino acids, which have long been problematic in peptide chemistry.

References and notes

1. (a) Dourtoglou, V.; Ziegler, J. C.; Gross, B. *Tetrahedron Lett.* **1978**, *19*, 1269–1272; (b) Dourtoglou, V.; Gross, B.; Lambropoulou, V.; Zioudrou, C. *Synthesis* **1984**, 572–574; (c) Knorr, R.; Trzeciak, A.; Bannwarth, W.; Gilleseen, D. *Tetrahedron Lett.* **1989**, *30*, 1927–1930.
2. Carpino, L. A. *J. Am. Chem. Soc.* **1993**, *115*, 4397–4398.
3. (a) Coste, J.; Le-Nguyen, D.; Castro, B. *Tetrahedron Lett.* **1990**, *31*, 205–208; (b) Frêrot, E.; Coste, J.; Pantaloni, A.; Dufor, M. N.; Jouin, P. *Tetrahedron* **1991**, *47*, 259–270.
4. Albericio, F.; Cases, M.; Alsina, J.; Triolo, S. A.; Carpino, L. A.; Kates, S. A. *Tetrahedron Lett.* **1997**, *38*, 4853–4856.
5. (a) El-Faham, A.; Albericio, F. *Org. Lett.* **2007**, *9*, 4475–4477; (b) El-Faham, A.; Funosas, R. S.; Prohens, R.; Albericio, F. *Chem. Eur. J.* **2009**, *15*, 9404–9416.
6. Dannecker-Dörig, L.; Linden, A.; Heimgartner, H. *Helv. Chim. Acta* **2011**, *94*, 993–1011.
7. Brückner, H.; Koza, A. *Amino Acids* **2003**, *24*, 311–323.
8. Carpino, L. A.; Imazumi, H.; El-Faham, A.; Ferrer, F. J.; Zhang, C.; Lee, Y.; Foxman, B. M.; Henklein, P.; Hanay, C.; Mügge, C. *Angew. Chem., Int. Ed.* **2002**, *41*, 441–445.
9. Unpublished data.
10. Shimizu, M.; Wada, T.; Saigo, K. *J. Org. Chem.* **2004**, *69*, 5261–5268.
11. Oka, N.; Shimizu, M.; Saigo, K.; Wada, T. *Tetrahedron* **2006**, *15*, 3667–3673.
12. Murata, A.; Wada, T. *Bioorg. Med. Chem. Lett.* **2006**, *16*, 2933–2936.
13. Toniolo, C.; Crisma, M.; Bonora, G. M.; Benedetti, E.; Di Blasio, B.; Pavone, V.; Pedone, C.; Santini, A. *Biopolymers* **1991**, *31*, 129–138.
14. Kubelka, J.; Silva, R. A. G. D.; Keiderling, T. A. *J. Am. Chem. Soc.* **2002**, *124*, 5325–5332.
15. Nagata, S.; Hamasaki, T.; Uetake, K.; Masuda, H.; Takagaki, K.; Oka, N.; Wada, T.; Ohgi, T.; Yano, J. *Nucleic Acids Res.* **2010**, *38*, 7845–7857.
16. Beaucage, S. L. In *Current Protocols in Nucleic Acid Chemistry*; John Wiley & Sons: New York, 2008; Vol. 1.; pp 30.1–3.17.21.
17. The reversed-phase HPLC analysis and purification of H-$(Aib)_4$-Tyr-NH_2 were carried out on a μBondasphere 5 μm C18 column (100 Å, 3.9 mm × 150 mm) (Waters) using 0.05% TFA/water at a linear gradient from 0% to 35% MeCN in 35 min at a flow rate of 0.5 ml/min. The characterization of H-$(Aib)_4$-Tyr-NH_2 was established by MALDI/TOF mass spectrometry, using 2,5-dihydroxybenzoic acid as a matrix. Calcd ($M+Na^+$): 543.30. Found: 543.16.
18. The reversed-phase HPLC analysis of Z-Phg-Pro-NH_2 was carried out on a μBondasphere 5 μm C18 column (100 Å, 3.9 mm × 150 mm) (Waters) using 0.05% TFA/water at a linear gradient from 30% to 45% MeCN in 30 min at a flow rate of 0.5 ml/min at 40 °C. The characterizations of Z-Phg-Pro-NH_2 and Z-D-Phg-Pro-NH_2 were established by co-injection with an authentic sample. t_{LL} = 15.5 min, t_{DL} = 16.8 min.

ORGANIC LETTERS

2013
Vol. 15, No. 23
5948–5951

Stereoselective Synthesis of *P*-Modified α-Glycosyl Phosphates by the Oxazaphospholidine Approach

Mihoko Noro,[†] Shoichi Fujita,[†] and Takeshi Wada*[,†,‡]

Department of Medical Genome Sciences, Graduate School of Frontier Sciences, The University of Tokyo, Bioscience Building 702, 5-1-5 Kashiwanoha, Kashiwa, Chiba 277-8562, Japan, and Department of Medicinal and Life Schience, Faculty of Pharmaceutical Sciences, Tokyo University of Science 2641, Yamazaki, Noda, Chiba 278-8510, Japan

twada@rs.tus.ac.jp

Received September 26, 2013

ABSTRACT

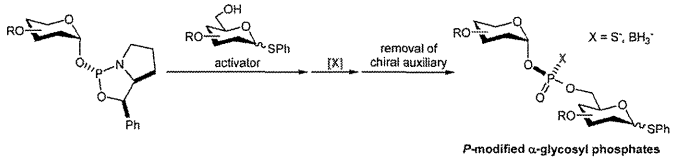

α-Glycosyl phosphate derivatives are widely known as constituents of biomolecules. To date, several types of non-natural α-glycosyl phosphates including "*P*-modified analogs" have been synthesized to investigate their characteristics. Herein a new approach to the stereoselective modification of the intersugar phosphorus atom in α-glycosyl phosphates by use of the oxazaphospholidine method is presented. Via this approach, the dimers of α-glycosyl phosphorothioates and α-glycosyl boranophosphates were obtained efficiently and stereoselectively.

α-Glycosyl phosphate derivatives are widely known as constituents of capsular polysaccharides in pathogenic bacteria such as *Neisseria meningitidis* and *Streptococcus pneumoniae*,[1,3] or the glycocalyx of parasitic protozoans such as *Leishmania* and *Trypanosoma*.[2,3]They have repeating units of phosphoglycans, many of which are considered to be important factors in biophenomena such as immunological responses and infection. Therefore, investigation of their roles as biomolecules is being carried out for the purpose of elucidating their biomechanisms and applying them in drug development.[1−3]

With such aims, several types of non-natural α-glycosyl phosphate analogs have been synthesized in previous studies.[4] Among them, we focused on the "*P*-modified analogs," where one of the nonbridging oxygen atoms is replaced by a different atom or a substituent. The intersugar phosphodiester linkage is considered to be an important factor affecting several biophenomena. Thus, *P*-modified analogs could become useful tools to clarify their biological modes of action. Moreover, the phosphodiester moiety is known to make a large contribution to chemical stability, and proper modification of the phosphorus atom is reported to further improve chemical stability.[5] For these reasons, *P*-modified glycosyl phosphate derivatives are considered promising analogs.

These molecules have a chiral center at the intersugar phosphorus atom. Because biological activity generally differs between stereoisomers, stereochemically controlled

[†] The University of Tokyo.
[‡] Tokyo University of Science.

(1) (a) Trotter, C. L.; McVernon, J.; Ramsay, M. E.; Whitney, C. G.; Mulholland, E. K.; Goldblatt, D.; Hombach, J.; Kieny, M.-P. *Vaccine* **2008**, *26*, 4434–4445. (b) Joshi, V. S.; Bajaj, I. B.; Survase, S. A.; Singhal, R. S.; Kennedy, J. F. *Carbohydr. Polym.* **2009**, *75*, 553–565.

(2) (a) Mendonça-Previato, L.; Todeschini, A. R.; Heise, N.; Agrellos, O. A.; Dias, W. B.; Previato, J. O. *Curr. Org. Chem.* **2008**, *12*, 926–939. (b) Mendonça-Previato, L.; Todeschini, A. R.; Heise, N.; Previato, J. O. *Curr. Org. Struct. Biol.* **2005**, *15*, 499–505. (c) Hansson, J.; Oscarson, S. *Curr. Org. Chem.* **2000**, *4*, 535–564.

(3) Nikolaev, A. V.; Botvinko, I. V.; Ross, A. J. *Carbohydr. Res.* **2007**, *342*, 297–344.

(4) (a) Routier, F. H.; Higson, A. P.; Ivanova, I. A.; Ross, A. J.; Tsvetkov, Y. E.; Yashunsky, D. V.; Bates, P. A.; Nikilaev, A. V.; Ferguson, M. A. J. *Biochemistry* **2000**, *39*, 8017–8025. (b) Singh, A. H.; Newborn, J. S.; Raushel, F. M. *Bioorg. Chem.* **1988**, *16*, 206–214. (c) Cohen, S. B.; Halcomb, R. L. *J. Org. Chem.* **2000**, *65*, 6145–6152. (d) Klinger, M. M.; McCarthy, D. J. *Bioorg. Med. Chem. Lett.* **1992**, *2*, 197–200. (e) Sheu, F. R.; Frey, P. A. *J. Biol. Chem.* **1978**, *253*, 3378–3380. (f) Yamazaki, Y.; Nagatsuka, Y.; Oshima, E.; Suzuki, Y.; Hirabayashi, Y.; Hashikawa, T. *J. Immunol. Methods* **2006**, *311*, 106.

(5) (a) Prosperi, D.; Panza, L.; Poletti, L.; Lay, L. *Tetrahedron* **2000**, *56*, 4811–4815. (b) Matsumura, F.; Oka, N.; Wada, T. *Org. Lett.* **2008**, *8*, 1557–1560.

10.1021/ol402785h
Published on Web 11/13/2013

Table 1. Preparation of Monomer Units

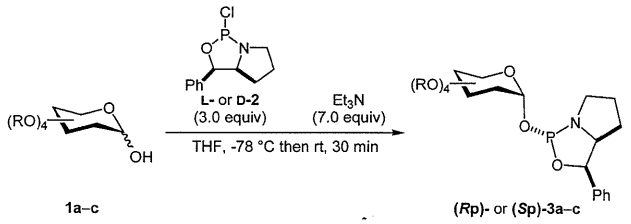

entry	2	product	R	Man/ Glc	yield (%)	diastereo ratio[a] *trans*: *cis*	α:β[b]
1	**L**	**(*Rp*)-3a**	Bn	Man	quant	>99:1	>99:1
2	**D**	**(*Sp*)-3a**	Bn	Man	74	>99:1	>99:1
3	**L**	**(*Rp*)-3b**	Bz	Man	90	>99:1	>99:1
4	**D**	**(*Sp*)-3b**	Bz	Man	83	>99:1	>99:1
5	**L**	**(*Rp*)-3c**	Bz	Glc	82	>99:1	95:5
6	**D**	**(*Sp*)-3c**	Bz	Glc	65	>99:1	>99:1

[a] Estimated by ^{31}P NMR. [b] For isolated product.

derivatives are required for assessment of their biological properties. However, stereoselective synthesis of *P*-modified glycosyl phosphates has not been accomplished yet.

Against such a background, we herein present a new approach to the stereoselective modification of the intersugar phosphorus atom with the "oxazaphospholidine method." This method has been used for the stereocontrolled synthesis of phosphorothioate DNA,[6a] RNA,[6b] and boranophosphate DNA[6c] for nucleic acid drugs. We applied this method to the synthesis of glycosyl phosphate analogs and first accomplished the stereocontrol of the intersugar phosphorus atom.

We prepared monomer units **(*Rp*)-** and **(*Sp*)-3a–c** as shown in Table 1. They were synthesized by the stereocontrolled phosphitylation of sugar derivatives bearing free anomeric hydroxyl groups with (4*S*,5*R*)- or (4*R*,5*S*)-2-chloro-1,3,2-oxazaphospholidine derivatives (L- or D-**2**), which were obtained by the reaction between PCl_3 and the corresponding 1,2-amino alcohols as previously reported.[4a] Mannopyranosyl monomers **(*Rp*)-** and **(*Sp*)-3a–b** were obtained in a highly α-selective manner because of the stereoelectronic effect of their axial 2-OH. As for glucopyranosyl derivatives, precursor **1c**, which was a mixture of α and β isomers, was recrystallized several times from AcOEt or CH_2Cl_2/hexane to obtain α-rich isomers. The isomers almost retained their stereochemical purity through the following phosphitylation step even though the reaction conditions could induce anomerization. This experimental fact suggests that phosphitylation of **1** was substantially more rapid than its anomerization.[7]

Using the synthesized monomer units, we attempted to synthesize stereoregulated *P*-modified dimers. In this study, as representative *P*-modified analogs, we selected boranophosphates and phosphorothioates to be the synthetic targets.

First, we describe the synthesis of glycosyl boranophosphates. We employed *O*-benzoyl-protected monomer units **(*Rp*)-** and **(*Sp*)-3b–c** because the benzyl groups could not be removed without associated deboronation of boranophosphodiester derivatives.[8]

Scheme 1. Synthesis of Glycosyl Boranophosphates

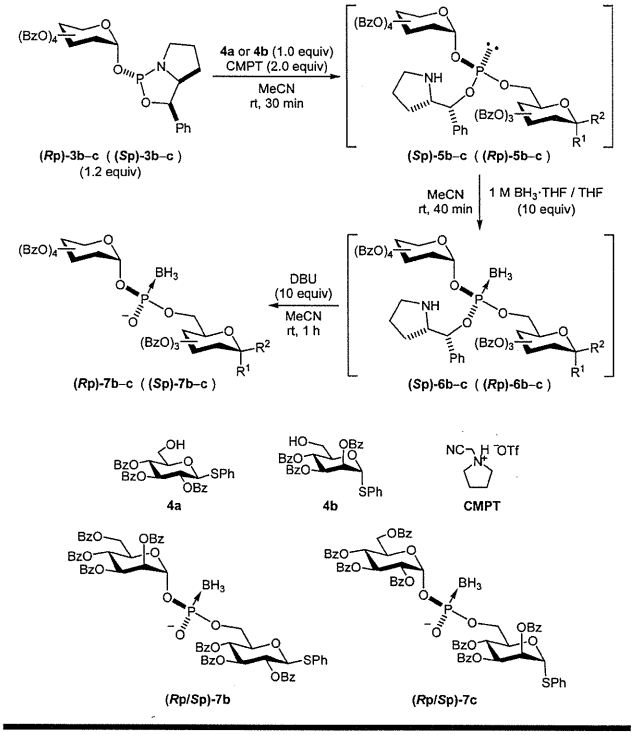

The *P*-modified dimers were synthesized via a three-step reaction in one pot (Scheme 1). The monomer units **(*Rp*)-** or **(*Sp*)-3b–c** were condensed with 1-*O*-thiophenyl-2,3,4-tri-*O*-benzoyl-β-D-glucopyranoside **4a** or 1-*O*-thiophenyl-2,3,4-tri-*O*-benzoyl-α-D-mannopyranoside **4b**, in the presence of *N*-(cyanomethyl)pyrrolidinium triflate (CMPT), which is an acid activator we developed for the stereospecific condensation of oxazaphospholidine monomers.[9] Then, the resultant diastereopure glycosyl phosphite intermediates **(*Sp*)-** or **(*Rp*)-5b–c** were boronated by treatment with 1 M BH_3·THF in THF to give the glycosyl boranophosphotriesters **(*Sp*)-** or **(*Rp*)-6b–c**.

In the last step, the removal of the chiral auxiliary was attempted in the presence of several basic reagents (Table 2). Each reaction was monitored by ^{31}P NMR, and it appeared that pyridine, 2,6-lutidine, and triethylamine (TEA) were not sufficiently basic to activate the nitrogen atom of the

(6) (a) Oka, N.; Yamamoto, M.; Sato, T.; Wada, T. *J. Am. Chem. Soc.* **2008**, *130*, 16031–16037. (b) Oka, N.; Kondo, T.; Fujiwara, S.; Maizuru, Y.; Wada, T. *Org. Lett.* **2009**, *11*, 967–970. (c) Wada, T.; Maizuru, Y.; Shimizu, M.; Oka, N.; Saigo, K. *Bioorg. Mol. Chem. Lett.* **2006**, *16*, 3111–3114.

(7) We observed that glucopyranosyl derivative **1** (α:β = 79:21) gave monomer unit **3** (α:β = 80:20) through this phosphitylation step.

(8) Unpublished data.

(9) (a) Oka, N.; Wada, T.; Saigo, K. *J. Am. Chem. Soc.* **2002**, *124*, 4962–4967. (b) Oka, N.; Wada, T.; Saigo, K. *J. Am. Chem. Soc.* **2003**, *125*, 8307–8317.

pyrrolidine ring of the chiral auxiliary and caused deboronation as a competitive side reaction. Although such a side reaction was not observed when using *N*,*N*-diisopropylethylamine (DIPEA), the intended reaction was not complete. In contrast, the chiral auxiliary was successfully removed by 1,8-diazabicyclo[5.4.0]undec-7-ene (DBU) in 5 min and glycosyl boranophosphodiester **7b** was quantitatively produced as a DBU salt. These results suggest that the main reaction should be rapid enough compared to deboronation in this case.

Table 2. Reaction Conditions for the Removal of Chiral Auxiliaries

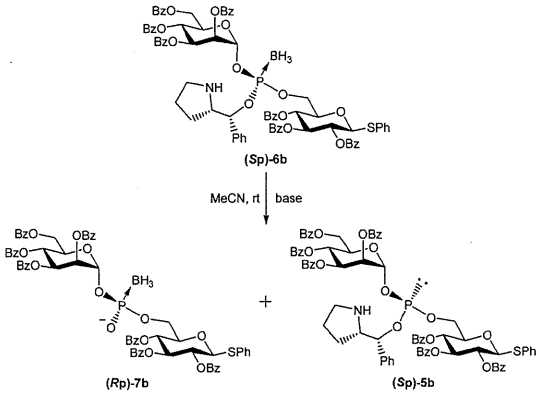

	reaction conditions			
entry	base	equiv	time	**6b**:**7b**:**5b**[a]
1	pyridine	10	overnight	–[b]
2	2,6-lutidine	20	overnight	85:0:15
3	TEA	30	overnight	8:77:15
4	DIPEA	10	overnight	29:71:0
5	DBU	10	1 h	0:100:0

[a] Estimated by ^{31}P NMR. [b] Not monitored.

Next, we describe the synthesis of glycosyl phosphorothioates (Scheme 2). It was performed by condensation of monomer units and sugar derivatives bearing free 6-OH, and the chiral auxiliaries were removed by the previously reported procedure.

In the sulfurization reaction of benzyl-protected glycosyl phosphites using *N*,*N*′-dimethylthiuram disulfide (DTD)[10] as a sulfurizing reagent, the formation of undefined byproducts was observed. Because it seemed to be caused by the decomposition of the *P*-activated intermediate, we changed the protecting group of the sugar hydroxyl moiety from a benzyl group to a benzoyl group, which destabilized the oxocarbenium cation. In addition, we tested other types of sulfurizing reagents such as POS[11] and S_8 whose sulfurizing reactions are expected to be more rapid than that of DTD.

The results are shown in Table 3. As we expected, the benzoyl-protected glycosyl phosphites were more efficiently

Scheme 2. Synthesis of Glycosyl Phosphorothioates

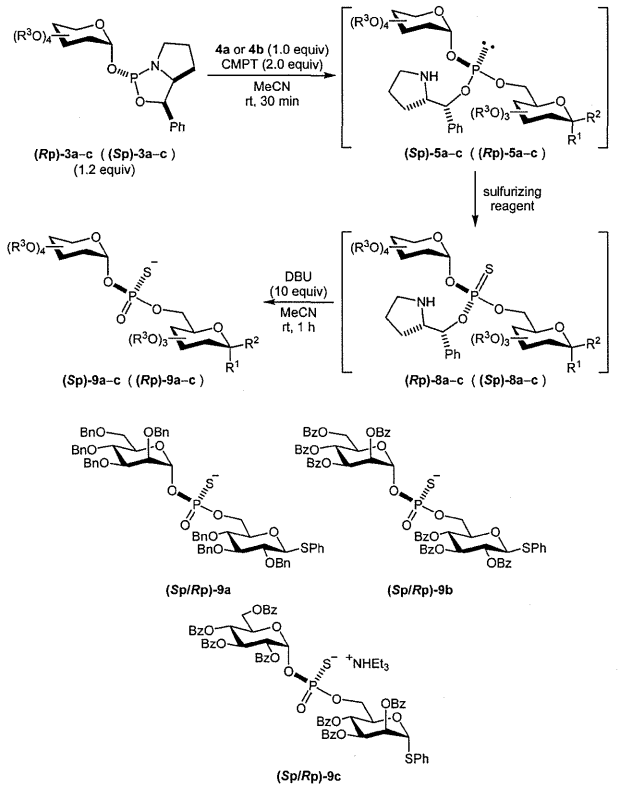

Table 3. Reaction Conditions for Sulfurization

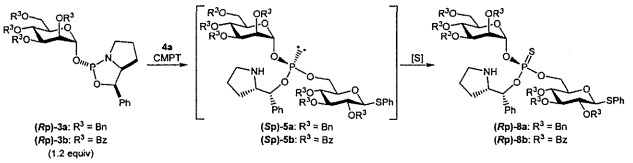

entry	R^3	sulfurizing reagents	product ratio of **8a**–**b**[a]	diastereo ratio[a]
1	Bn	DTD	46%	–[b]
2	Bn	POS	80%	–[b]
3	Bn	S_8	quant	>99:1
4	Bz	DTD	87%	–[b]
5	Bz	POS	quant	>99:1
6	Bz	S_8	quant	>99:1

[a] Estimated by ^{31}P NMR. [b] Not determined.

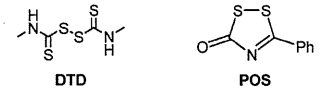

transformed into the corresponding glycosyl phosphorothioate triesters than the benzyl-protected compounds. In addition, both of the alternative sulfurizing reagents improved

(10) Song, Q.; Wang, Z.; Sanghvi, Y. S. *Nucleosides, Nucleotides, Nucleic Acids* **2003**, *22*, 629–633.
(11) Roy, S. K.; Tang, J. Y. U.S. Patent 6, 500, 944, 2002.

Table 4. Stereocontrolled Synthesis of Dimers of Glycosyl Boranophosphate and Phosphorothioate Derivatives

entry	target compounds		yield	diastereo ratio[a] (*R*p:*S*p)
1	(*R*p)-Man-PB-Glc	**(*R*p)-7b**	79%	>99:1
2	(*S*p)-Man-PB-Glc	**(*S*p)-7b**	76%	>1:99
3	(*R*p)-Glc-PB-Man	**(*R*p)-7c**	77%	>99:1
4	(*S*p)-Glc-PB-Man	**(*S*p)-7c**	96%	>1:99
5	(*R*p)-Man-PS-Glc	**(*R*p)-9b**	82%	>99:1
6	(*S*p)-Man-PS-Glc	**(*S*p)-9b**	80%	>1:99
7	(*R*p)-Glc-PS-Man	**(*R*p)-9c**	77%	>99:1
8	(*S*p)-Glc-PS-Man	**(*S*p)- 9c**	73%	>1:99

[a] Estimated by ^{1}H or ^{31}P NMR.

this step and the formation of byproducts was reduced compared to the reaction using DTD.

On the basis of these results, we synthesized eight types of *P*-modified glycosyl phosphate dimers. The structure of α-D-Glc-(1-*P*-6)-D-Man is a fragment of glycocalyx lipophosphoglycans of *Leishmania*. The results are shown in Table 4.

In conclusion, we successfully accomplished an efficient and highly stereoselective synthesis of glycosyl boranophosphates and glycosyl phosphorothioates in different combinations of sugar moieties. These results suggest that this method could be a versatile approach to the synthesis of a wide variety of *P*-modified glycosyl phosphate analogs. In addition, this method is expected to be applicable to solid-phase synthesis, which can enable the synthesis of oligoglycosyl phosphate analogs.

Supporting Information Available. Experimental details and characterization data, including ^{1}H, ^{13}C, and ^{31}P spectra. This material is available free of charge via the Internet at http://pubs.acs.org.

The authors declare no competing financial interest.

analytical chemistry

Article

pubs.acs.org/ac

A Protein–Protein Interaction Assay Based on the Functional Complementation of Mutant Firefly Luciferases

Yuki Ohmuro-Matsuyama,[†,‡,∥] Kota Nakano,[†] Aoi Kimura,[†] Keiichi Ayabe,[†] Masaki Ihara,[§] Takeshi Wada,[⊥] and Hiroshi Ueda*[,†,‡,§]

[†]Department of Chemistry and Biotechnology, School of Engineering, The University of Tokyo, 7-3-1 Hongo, Bunkyo-ku, Tokyo 113-8656, Japan

[‡]Chemical Resources Laboratory, Tokyo Institute of Technology, 4259-R1-18 Nagatsuta-cho, Midori-ku, Yokohama 226-8503, Japan

[∥]The Japan Society for the Promotion of Science, 8 Ichiban-Cho, Chiyoda-ku, Tokyo 102-8472, Japan

[§]Department of Bioengineering, School of Engineering, The University of Tokyo, 7-3-1 Hongo, Bunkyo-ku, Tokyo 113-8656, Japan

[⊥]Department of Medical Genome Sciences, Graduate School of Frontier Sciences, The University of Tokyo, 5-1-5 Kashiwano-ha, Kashiwa, Chiba 277-8562, Japan

Supporting Information

ABSTRACT: We report a novel bioluminescent protein–protein interaction (PPI) assay, which is based on the functional complementation of two mutant firefly luciferases (Fluc). The chemical reaction catalyzed by Fluc is divided into two half reactions of ATP-driven luciferin adenylation and subsequent oxidative reactions. In the former adenylation half-reaction, a luciferyl-adenylate (LH_2-AMP) intermediate is produced from LH_2 and ATP. With this intermediate, the latter oxidative reactions produce oxyluciferin via proton abstraction at the C4 carbon of LH_2-AMP. We created and optimized two Fluc mutants; one is named "Donor", which virtually lacks oxidative activity, while the other, named "Acceptor", is almost defective in the adenylation activity. Then, the two mutants are fused to interacting partners, and prepared as pure proteins. When the interaction between the partners is induced, higher efficiency of LH_2-AMP transfer between the Donor and Acceptor enzymes resulted in increased luminescence. The assay was found to work both *in vitro* and in cultured cells with strong signals. This would be the first example of reconstituting two divided reactions of one enzyme to detect PPI, which will not only be utilized as a robust PPI assay, but also open a way to control the activity of similar enzymes in acyl/adenylate-forming enzyme superfamily.

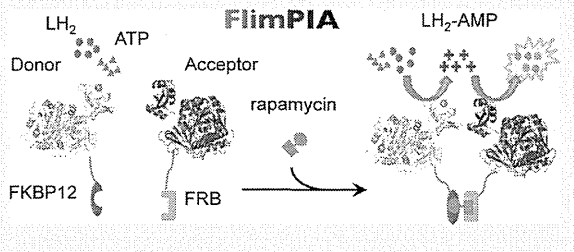

The human interactome is predicted to contain 150 000 to 300 000 protein–protein interactions (PPIs).[1,2] There is a significant focus on detecting and assaying PPIs in biology and biotechnology as these interactions are essential in many important cellular functions, and their dysregulation causes diseases. To discover and investigate PPI, exploration of PPI assays is considered highly important. Firefly luciferase (Fluc) is frequently used as a reporter in high-throughput screening assays and also in PPI assays, owing to the exceptional sensitivity, dynamic range, and rapid measurement that bioluminescence affords. As a PPI assay, protein-fragment complementation assay (PCA) is a simple and user-friendly method, and Fluc-based PPI assay shows an excellent property especially in the cellular milieu.[3−5] However, it is also revealed that purified Fluc-based PCA probes are relatively unstable and cannot endure longer incubation *in vitro*.[5] To overcome this limitation, here we explored a novel PPI assay based on the functional complementation of two Fluc mutants.

Fluc is a monooxygenase that produces excited state oxyluciferin (OxL) from firefly D-luciferin (LH_2) by multistep catalysis (Figure 1a). The reactions can be divided into two half-reactions, ATP-driven luciferin adenylation and subsequent oxidative reactions, which are catalyzed by two different protein conformations.[6,7] In the former adenylation half-reaction, a luciferyl-adenylate (LH_2-AMP) intermediate is produced from LH_2 and ATP. With this intermediate, the latter oxidative reactions produce OxL via proton abstraction at the C4 carbon of LH_2-AMP. To date, the contribution of several key amino acid residues to each catalytic step has been revealed. According to crystal structural studies,[8,9] Fluc is composed of a large N-terminal domain (1–437 aa, N-domain) and a smaller C-terminal domain (441–550 aa, C-domain) connected by a flexible hinge; the active site is surrounded by the residues mainly located at the N-domain including H245, except for a few residues in the C-domain.[10] In the C-domain, K529 is considered a key residue for the adenylation reaction,[11] while K443 is essential in the oxidative luminescent reaction steps.[12] In addition, we have found that another key residue mutant

Received: June 6, 2013
Accepted: July 5, 2013
Published: August 1, 2013

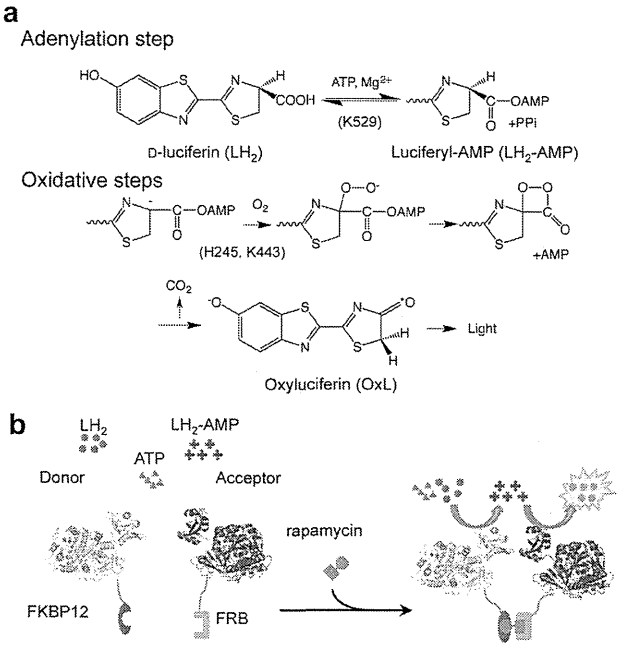

Figure 1. Principle of FlimPIA (firefly luminescent intermediate-based protein interaction assay). (a) Chemical reactions catalyzed by firefly luciferase (Fluc). Fluc produces excited state oxyluciferin (OxL) from D-luciferin (LH_2) by a two-step catalysis: the adenylation step and the oxidative steps. (b) Schematic representation of FlimPIA. Fluc (Donor) exhibits low effectiveness in the oxidative steps, while Fluc (Acceptor) exhibits low effectiveness in the adenylation step. FKBP12 (FK506-binding protein 12) and FRB (FKBP-rapamycin-associated protein) interact in the presence of rapamycin. The two mutants were each fused with one of the interacting partners, respectively. LH_2-AMP (luciferyl-adenylate) produced by the Donor is oxidized by the Acceptor, which results in stronger light emission upon interaction.

(H245D) produces a large amount of LH_2-AMP outside of the enzyme, presumably because of its low oxidation activity.[13] Motivated by these findings, we attempted to make a novel enzyme proximity detection assay mediated by the reaction intermediate LH_2-AMP.

EXPERIMENTAL SECTION

Materials. ATP and D-luciferin (LH_2) were from Sigma, St. Louis, MO. Synthesis and purification of LH_2-AMP were performed according to Ayabe et al.[13] MOPS (3-(*N*-morpholino)propanesulfonic acid) was from Dojindo, Kumamoto, Japan. Rapamycin was from Wako Pure Chemical Industries, Osaka, Japan or LKT Laboratories, St. Paul, MN. FK506 was from Enzo Laboratories, Switzerland. Oligonucleotides were from Fasmac Co., Kanagawa, Japan. Synthetic genes for *Escherichia coli* codon-optimized human FKBP12 and FRB, appended with *NcoI*/*SfiI* and *NotI* sites at the 5′ and 3′ ends, respectively, were from Mr Gene GmbH, Regensburg, Germany. The plasmid pFH154 encoding human fibronectin cDNA was from Health Science Research Resources Bank (HSRRB), Osaka, Japan. Other reagents in the highest grade available were from Wako Pure Chemical Industries unless otherwise indicated.

Construction of FKBP/FRB Fused Fluc Expression Vectors. The DNA fragment encoding Fluc was obtained by PCR using pGEX-Ppy vector[14] as a template, and primers LucNotG4SB (5′-gg cgc gcc GCG GCC GCC GGT GGT GGT GGT AGC ATG GAA GAC GCC AAA AAC ATA AAG-3′) encoding a G_4S linker and *NotI* site (underlined) and LucXhoF (5′-g gcg cgc CTC GAG CTT TCC GCC CTT CTT GGC CT-3′) containing *XhoI* site (underlined). Similarly, N- and C-terminal domain genes were amplified with primers LucNotG4SB and Luc437XhoF (5′-g gcg cgc CTC GAG GCG GTC AAC TAT GAA GAA GTG-3′), and Luc394NotG4SB (5′-gg cgc gcc GCG GCC GCC GGT GGT GGT GGT AGC GGA CCT ATG ATT ATG TCC GG-3′) and LucXhoF, respectively. The amplified fragments were cloned into pET32b (Merck, Darmstadt, Germany) between the *NotI* and *XhoI* sites, to give pET32/Fluc, pET32/FlucN, and pET32/FlucC, respectively. The synthetic genes encoding FKBP12 and FRB (binding domains, BDs) cDNAs were digested with *NcoI* and *NotI*, and the digested fragments were inserted in pET32/Fluc, pET32/FlucN, and pET32/FlucC digested with the same enzymes, to give pET32/BD/Fluc, pET32/BD/FlucN, and pET32/BD/FlucC, respectively.

Construction of Fluc Mutant Expression Vectors. With the use of pET32/BD/Fluc, QuikChange site-directed mutagenesis with *Pfu-Ultra* DNA polymerase (Stratagene, Agilent) was performed to make H245D, K443A, K529A mutants and their combinations. Mutagenesis was carried out according to the manufacturer's instruction using the following oligonucleotides and their complementary strands as primers: for H245D, 5′-GTT CCA TTC CAT GAC GGT TTT GGA ATG T-3′; for K443A, 5′-GAC CTC TTG AAG TCT TTA ATT GCA TAC AAA GGA TAT CAG GTG GC-3′; and for K529A, 5′- CCG AAA GGT CTT ACC GGA GCT CTC GAC GCA AGA AAA ATC AGA GAG-3′.

With the use of pET32/BD/Fluc(H245D/K443A) and pET32/BD/Fluc(K529A) as templates, QuikChange site-directed mutagenesis was performed to make H245D/E354K/K443A/L530R (Donor) and E354K/K529Q (Acceptor) Fluc mutant genes, respectively, using the following oligonucleotides and their complementary strands as primers: for E354K, 5′-TTC TGA TTA CAC CCA AGG GGG ATG ATA AA-3′; for L530R, 5′-CCG AAA GGT CTT ACC GGT AAA CGC GAC GCA AGA AAA ATC A-3′; and for K529Q, 5′-CCG AAA GGT CTT AC GGT CRR CTC GAC GCA AGA AAA TCA GAG AG-3′. To express Donor and Acceptor without BD sequence, the mutant Fluc genes were amplified with primers Nco-GGGGS-LucBack (5′-gga att CCA TGG GTG GTG GTG GTA GCA TGG-3′) and T7term (5′-TAG TTA TTG CTC AGC GGT GG-3′), digested with *NcoI* and *XhoI*, and inserted to the vector digested with the same enzymes to give pET32/Donor and pET32/Acceptor. The nucleotide sequences were confirmed by CEQ-8000 sequencer using CEQ DTCS kit (Beckman-Coulter, Tokyo, Japan).

The vectors for mammalian expression were made based on pcDNA3.1/hygro(+) (Invitrogen, Life Technologies). First, the *XbaI*–*XhoI* fragment encoding *E. coli* maltose binding protein (MBP) and antibody V_H fragment for bisphenol A was obtained from pET-MBP-V_H(BPA),[15] and inserted between *NheI* and *XhoI* sites of pcDNA3.1/hygro(+), designated pcMBP-V_H/hygro. The *SfiI*–*XhoI* fragment encoding either FKBP12 or FRB (binding domain, BD) and a mutant luciferase was obtained from a corresponding *E. coli* expression vector, and inserted to pcMBP-V_H/hygro digested by the same enzymes, to yield a mammalian expression vector for MBP-BD-Fluc mutant.

Expression and Purification of BD-Fused Fluc Mutants. The thioredoxin (Trx)-fused BD-Fluc mutant fusion

dx.doi.org/10.1021/ac4016825 | *Anal. Chem.* 2013, 85, 7935–7940

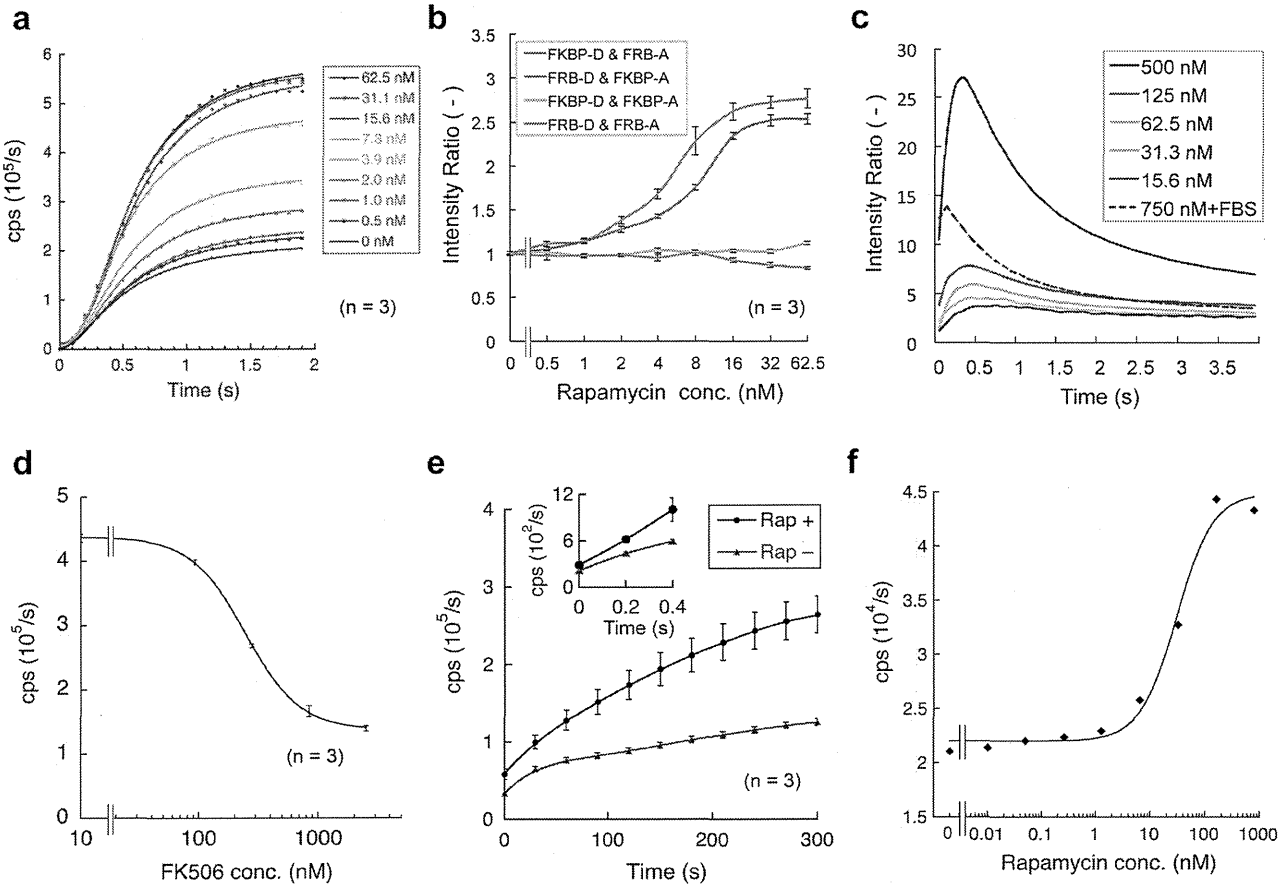

Figure 2. FlimPIA in *vitro* (a–d) and in cultured cells (e–f). (a) Luminescence time course at several rapamycin concentrations. A mixture of FKBP/Donor and FRB/Acceptor (50 nM each) was used. (b) Specific detection of FKBP12-FRB interaction. The four possible combinations of two Fluc mutants, namely, FRB/Donor and FKBP/Acceptor (50 nM each) were tested for their rapamycin dose-dependency. The relative luminescence integrated for 1.5–1.6 *s* after substrate addition is shown. (c) Time course of S/B (signal/background) ratio obtained with the mixture of FKBP/Donor and FRB/Acceptor with and without equimolar rapamycin. The ratio of the two light intensities at the indicated time point is shown. Sample with 40% fetal bovine serum and 750 nM proteins is also shown. (d) Competition of PPI (protein–protein interaction) by FK506. Rapamycin (80 nM) and FK506 at indicated concentration were added to the mixture of FKBP/Donor and FRB/Acceptor (80 nM each). The luminescence integrated for 0.8–0.9 s after substrate addition is shown. (e) Luminescence time course of 293T cells transfected with FKBP/Donor and FRB/Acceptor expression vectors with or without 100 nM rapamycin (1.2×10^4 cells/well). Inset shows the measurements at the early time points. The averages of three measurements are shown with 1 SD. (f) Rapamycin dose dependency of the luminescence emitted by 293T cells transfected with the same vectors (4×10^3 cells/well) measured 10 min after LH_2 addition. Error bars, s.d.

protein was expressed in *E. coli* BL21 (pLysS, DE3) (Novagen) as a histidine tagged protein. To purify the expressed fusion protein, Talon metal affinity resin (Clontech) was used according to the manufacturer's instruction. Concentration of the purified protein was determined by CBB-stained SDS-PAGE co-loaded with various concentrations of BSA as a standard. The protein added with 15% of glycerol was stored at −80 °C before use.

Detection of FKBP12-FRB Interaction *in Vitro*. Rapamycin with or without FK506 was suspended in 100 mM MOPS, 10 mM $MgSO_4$, pH 7.3. The mixture (50 μL each) was dispensed to a well of 96-well half-area white plate (3693, Corning-Costar). The light intensity was measured after injection of 50 μL of 2× substrate solution (100 mM MOPS, 10 mM of $MgSO_4$, 20 mM ATP, and 150 μM luciferin, pH 7.3) with a periodical integration of 0.1 s with a luminometer AB-2350 with Phelios software (ATTO, Tokyo, Japan). Alternatively, the sample (50 μL) was placed in a tube, and 500 μL of substrate solution was added in a tube-based luminometer NU-2600 (Microtech Nichion, Chiba, Japan) under stirring. To detect the interaction in serum, equimolar mixture of the enzymes and rapamycin was suspended in 40% (v/v) fetal bovine serum (FBS, Life Technologies) in PBS. Light intensity was measured as above with 2× substrate solution containing 40% FBS.

Detection of FKBP12-FRB Interaction in Cultured Cells. Cos-7 and 293T cells were grown in Dulbecco's modified Eagle's medium (DMEM, Wako) supplemented with 10% FBS and Antibiotic-Antimycotic (Gibco). The cells were cultured at 37 °C in an air containing 5% CO_2 atmosphere with constant humidity. Transfection was carried out using Lipofectamine 2000 (Invitrogen) according to the manufacturer's instruction. Twenty-four hours after transfection, the cells were harvested with trypsin. The collected cell suspension was diluted (8×10^4 to 2.4×10^5 cells/mL) with DMEM without phenol red, aliquoted to 50 μL, added with rapamycin/FK506 as indicated, and dispensed into a well of 96-well white plate. The light intensity was measured with a periodical

dx.doi.org/10.1021/ac4016825 | *Anal. Chem.* 2013, 85, 7935–7940

integration of 1 s after injection of 50 μL DMEM containing 1.5 μM luciferin.

Detection of Mdm2-p53 Interaction. The transactivation domain gene of p53 (Residue 15−29)[16] was made by thermal cycling using following oligonucleotides with a restriction site (underlined): p53NcoBack (5′-gg aat tCC ATG GCT AGT CAG GAA ACA TTT TCA GAC CTA TGG AAA C-3′) and p53NotFor (5′-g gaa ttc tGC GGC CGC GTT TTC AGG AAG TAG TTT CCA TAG GTC TG-3′). Mdm2 gene (Residue 17−125) was obtained by PCR with human mdm2 gene as a template and mdm2NcoBack (5′-gg aat tCC ATG GCT TCG GAA CAA GAG ACC C-3′) and mdm2NotFor (5′-g gaa ttc tGC GGC CGC CTG CTG ATT GAC TAC TAC C-3′) as primers. The amplified fragments were digested with *Nco*I and *Not*I, and inserted to pET32/FRB-Fluc mutant vectors digested with the same enzymes. The proteins were expressed and purified as above, and used for FlimPIA *in vitro*.

RESULT AND DISCUSSION

Construction of Fluc Mutants with Impaired Half Reactions. To make an enzyme proximity detection assay mediated by the reaction intermediate LH_2-AMP, we combined the two mutations, H245D and K443A, to make a "Donor" of LH_2-AMP that retains high adenylation activity but lacks most of the oxidation activity. Additionally, we chose mutants of K529 as "Acceptors" of LH_2-AMP. To optimize the "Donor" Fluc mutant H245D/K443A, we introduced the L530R mutation,[17] which stabilizes bound ATP. This mutation resulted in a 3-fold increase in the production of LH_2-AMP, accompanied by only a small increase in oxidative luminescent activity (Figure S-1, Supporting Information). In addition, as a result of K529 mutant optimization, K529Q was chosen as a better "Acceptor" of LH_2-AMP, because the mutant showed higher activity than K529A over a wider LH_2 concentration range (Figure S-2, Supporting Information). In addition, the E354K mutation was introduced to all enzymes for enhanced thermostability.[18] Thus, we employed the H245D/E354K/K443A/L530R mutant ("Donor"), which provides the reaction intermediate LH_2-AMP, and the E354K/K529Q mutant ("Acceptor"), which utilizes the LH_2-AMP thereby produced. When the distance of these enzymes is large, the luminescent intensity will be at the background level because of inefficient transfer of LH_2-AMP between them. However, when the distance is shorten by the interaction between them, the luminescence derived of more abundant LH_2-AMP around the enzymes (detectable at nanomolar level[19]) will exceed the background luminescence (Figure 1b).

Detection of FKBP12-FRB Interaction. To apply these mutant Flucs to a PPI assay *in vitro*, each enzyme was fused with a well-known interacting protein pair, namely, FK506-binding protein 12 (FKBP12) and FKBP-rapamycin-associated protein (FRB), which associate in an antibiotic rapamycin-dependent manner.[20−22] The fusion proteins were expressed in *E. coli* and readily prepared as pure proteins. To assay the interaction, 50 nM each of purified FKBP12/Donor and FRB/Acceptor were mixed, and added with different concentrations of rapamycin up to 62.5 nM (Figure 2a, Figure S-3, Supporting Information). After adding the substrates LH_2 and ATP, the luminescent intensity was measured using a multiwell luminometer and it was found to increase immediately in a rapamycin concentration-dependent manner. This increase in luminescent intensity was rapid and it became steady at 1.5 s after the beginning of the reaction. When we used a tube-based luminometer with larger amounts of substrate, the increase in luminescent intensity continued up to 1 min, giving a good dose−luminescent intensity increment response (Figure S-3, Supporting Information).To see if the observed signal is the result of specific FKBP12−FRB interaction, other combinations of interacting protein/reporter pairs were also prepared, and examined for their responses (Figure 2b). Although the luminescent intensities of the cognate pairs having both FKBP12 and FRB showed rapamycin-dependent increase, the intensities for the pairs having FKBP12 or FRB alone did not show the response. The EC_{50} values for the cognate pairs were 10.2 ± 0.6 and 16.0 ± 2.1 nM, which corresponded well with the reported K_d of the FKBP/rapamycin interaction with FRB *in vitro*.[23] These results clearly indicate that a specific PPI is detected by this assay (named FlimPIA: firefly luminescent intermediate-based protein interaction assay) with sufficient response both in time and in magnitude.

To further confirm the specificity of FlimPIA, the Donor and Acceptor without interacting domains were prepared, and measured for their luminescent activity alone or in pairs (Figure S-4, Supporting Information). The result clearly shows that in the absence of interaction, the signal was just the arithmetic sum of each light emission, even if they are mixed together.

The magnitude of the signal/background (S/B) ratio is a key factor in determining the utility of the PPI assay. In the assay using FKBP-Donor and FRB-Acceptor, the S/B ratio increased according to the increased concentration of each protein, in response to equimolar rapamycin (Figure 2c and Figure S-4, Supporting Information). The resultant S/B ratio depended on the concentration of interacting proteins, and it reached as high as 27 within 0.5 s after the beginning of the reaction, at a protein/rapamycin concentration of 500 nM each. However, significant responses of >3.6-fold were observed at this time point for lower concentration of 15.6 nM.

For *in vitro* diagnostics, the applicability of the assay to clinical samples is very important. Therefore, the assay was performed in 40% fetal bovine serum (FBS) diluted with phosphate-buffered saline (PBS) (Figure 2c, dotted line). The mixture containing 750 nM each of FKBP12-Donor and FRB-Acceptor, with or without rapamycin, displayed an S/B ratio of more than 10 after 0.2 s following the addition of substrates LH_2 and ATP. In spite of some inhibition, possibly due to increased LH_2-AMP degradation and reduced diffusion, the result suggests the potential usefulness of FlimPIA in clinical diagnostics.

With this system, the effect of PPI inhibitor FK506 on the FKBP-FRB interaction was investigated. FK506, a strong macrolide immunosuppressant, binds to the same surface of FKBP12 as rapamycin.[21] As expected, when FK506 was added to the equimolar mixture (80 nM each) of FKBP-Donor, FRB-Acceptor, and rapamycin, dose-dependent reduction in luminescent intensity was observed, with an IC_{50} of 240 ± 5 nM. This agreed well with the reported inhibition curve[24] (Figure 2d).

Because the probes for this assay comprise protein, in theory, FlimPIA can be conducted with the probes expressed in the cells. To demonstrate this possibility, both FKBP-Donor and FRB-Acceptor proteins were transiently expressed as maltose binding protein-fusion proteins in cultured 293T cells, and the cells were treated with rapamycin. After adding LH_2 to the medium, the luminescent intensity of the transfected cells increased gradually for several minutes in a rapamycin-dependent manner (Figure 2e). In addition, the increase of

dx.doi.org/10.1021/ac4016825 | *Anal. Chem.* 2013, 85, 7935−7940

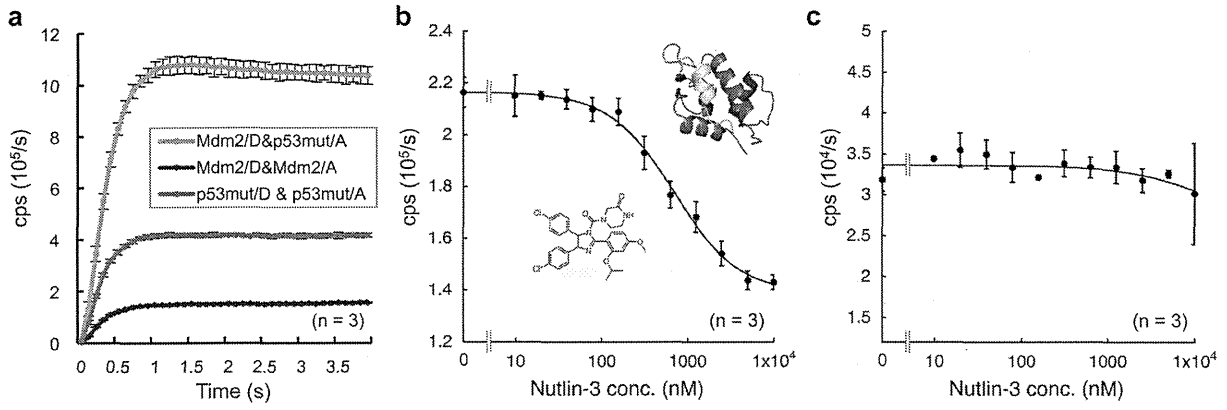

Figure 3. Detection of p53 peptide-Mdm2 interaction. (a) Luminescence time course of the cognate (Mdm2/Donor and p53/Acceptor) and control pairs (25 nM each). (b) Competition of PPI by a specific inhibitor. Nutlin-3 (bottom) at indicated concentration was added to the mixture of p53/Donor and Mdm2/Acceptor (25 nM each). The luminescence integrated for 0.8–0.9 s after substrate addition is shown. The ribbon model of Mdm2 (purple)-p53 peptide (light green) complex is also shown. (c) Nutlin-3 dose-dependency assayed with FKBP/Donor and FRB/Acceptor (25 nM each). The condition is the same as in (b). Error bars, s.d.

luminescent intensity was observed within 0.4 s after LH_2 addition (Figure 2e inset). The rapamycin dose-dependency of the luminescence was also determined, with a calculated EC_{50} of 30 ± 7 nM (Figure 2f). The higher EC_{50} than the value measured *in vitro* is probably due to slow diffusion of rapamycin. In addition, the luminescent intensity of Cos-7 cells transfected with the same vectors also showed rapamycin dependency (Figure S-5a, Supporting Information). In 293T cells, the inhibition of PPI by FK506 was also observed at higher dose than *in vitro*, probably reflecting the higher EC_{50} for rapamycin in this condition (IC_{50} = 727 ± 205 nM) (Figure S-5b, Supporting Information).

Detection of p53-Mdm2 Interaction. To show the generality of FlimPIA, detection of another PPI between a p53-derived peptide and Mdm2 was investigated. The Mdm2 oncoprotein is a cellular inhibitor of the p53 tumor suppressor in that it can bind the transactivation domain of p53 and downregulate its ability to activate transcription.[16] In certain cancers, mdm2 amplification is a common event and contributes to the inactivation of p53. When human mdm2 gene, as well as a high affinity Mdm2-binding region peptide of p53,[25] was each tethered to Donor and Acceptor enzyme, respectively, we could observe a higher signal than the control pairs with p53 peptide or Mdm2 tethered to both Donor and Acceptor (Figure 3a). In addition, the signal obtained with 25 nM each of Mdm2-Donor and p53-Acceptor was inhibited by a p53-Mdm2 interaction inhibitor Nutlin-3 (Alexis, mw, 581.5) (Figure 3b). On the contrary, no significant inhibition was observed for FKBP-Donor/FRB-Acceptor pair (Figure 3c). Taken together, the result suggests the potential of FlimPIA in the detection of various PPIs, as well as the validation and possibly screening of small molecule PPI inhibitors.

■ CONCLUSIONS

We developed an unconventional PPI assay by splitting not the enzyme-coding polypeptide but the compensating catalytic steps of Fluc enzyme. Because of its utility *in vitro*, the methodology will find various applications in basic biology, drug screening and clinical diagnostics. In addition, it will open a way to control the activity of similar enzymes in acyl/adenylate-forming enzyme superfamily, which include the enzymes catalyzing fatty acid metabolism and nonribosomal protein synthesis. Hopefully, the methodology will become a novel tool in metabolic engineering.

■ ASSOCIATED CONTENT

Ⓢ Supporting Information

Supplementary figures as noted in text are provided. This material is available free of charge via the Internet at http://pubs.acs.org.

■ AUTHOR INFORMATION

Corresponding Author

*Phone/Fax: +81-45-924-5248. E-mail: ueda@res.titech.ac.jp.

Notes

The authors declare no competing financial interest.

■ ACKNOWLEDGMENTS

We are indebted to T. Wakabayashi, Y. Husimi, T. Okabe, H. Kojima, and T. Nagano for their valued advice. We also thank B. Branchini for providing inspiration for the project, Yukiko Gotoh for human mdm2 cDNA. M.I. was supported by Fujifilm Co. Y.O.-M. was supported by SENTAN, JST, Japan, and partly by the "Leave a Nest" Microtech Nichion award.

■ REFERENCES

(1) Venkatesan, K.; Rual, J.-F.; Vazquez, A.; Stelzl, U.; Lemmens, I.; Hirozane-Kishikawa, T.; Hao, T.; Zenkner, M.; Xin, X.; Goh, K.-I.; Yildirim, M. A.; Simonis, N.; Heinzmann, K.; Gebreab, F.; Sahalie, J. M.; Cevik, S.; Simon, C.; de Smet, A.-S.; Dann, E.; Smolyar, A.; Vinayagam, A.; Yu, H.; Szeto, D.; Borick, H.; Dricot, A.; Klitgord, N.; Murray, R. R.; Lin, C.; Lalowski, M.; Timm, J.; Rau, K.; Boone, C.; Braun, P.; Cusick, M. E.; Roth, F. P.; Hill, D. E.; Tavernier, J.; Wanker, E. E.; Barabasi, A.-L.; Vidal, M. *Nat. Methods* **2009**, *6*, 83–90.

(2) Zhang, Q. C.; Petrey, D.; Deng, L.; Qiang, L.; Shi, Y.; Thu, C. A.; Bisikirska, B.; Lefebvre, C.; Accili, D.; Hunter, T.; Maniatis, T.; Califano, A.; Honig, B. *Nature* **2012**, *490*, 556–560.

(3) Michnick, S. W.; Ear, P. H.; Manderson, E. N.; Remy, I.; Stefan, E. *Nat. Rev. Drug Discovery* **2007**, *6*, 569–582.

(4) Porter, J. R.; Stains, C. I.; Jester, B. W.; Ghosh, I. *J. Am. Chem. Soc.* **2008**, *130*, 6488–6497.

(5) Ohmuro-Matsuyama, Y.; Chung, C.-I.; Ueda, H. *BMC Biotechnol.* **2013**, *13*, 31.

(6) Branchini, B. R.; Rosenberg, J. C.; Fontaine, D. M.; Southworth, T. L.; Behney, C. E.; Uzasci, L. *J. Am. Chem. Soc.* **2011**, *133*, 11088–11091.
(7) Sundlov, J. A.; Fontaine, D. M.; Southworth, T. L.; Branchini, B. R.; Gulick, A. M. *Biochemistry* **2012**, *51*, 6493–6495.
(8) Conti, E.; Franks, N. P.; Brick, P. *Structure* **1996**, *4*, 287–298.
(9) Nakatsu, T.; Ichiyama, S.; Hiratake, J.; Saldanha, A.; Kobashi, N.; Sakata, K.; Kato, H. *Nature* **2006**, *440*, 372–376.
(10) Gulick, A. M. *ACS Chem. Biol.* **2009**, *4*, 811–827.
(11) Branchini, B. R.; Murtiashaw, M. H.; Magyar, R. A.; Anderson, S. M. *Biochemistry* **2000**, *39*, 5433–5440.
(12) Branchini, B. R.; Southworth, T. L.; Murtiashaw, M. H.; Wilkinson, S. R.; Khattak, N. F.; Rosenberg, J. C.; Zimmer, M. *Biochemistry* **2005**, *44*, 1385–1393.
(13) Ayabe, K.; Zako, T.; Ueda, H. *FEBS Lett.* **2005**, *579*, 4389–4394.
(14) Kitayama, A.; Yoshizaki, H.; Ohmiya, Y.; Ueda, H.; Nagamune, T. *Photochem. Photobiol.* **2003**, *77*, 333–338.
(15) Sakata, T.; Ihara, M.; Makino, I.; Miyahara, Y.; Ueda, H. *Anal. Chem.* **2009**, *81*, 7532–7537.
(16) Kussie, P. H.; Gorina, S.; Marechal, V.; Elenbaas, B.; Moreau, J.; Levine, A. J.; Pavletich, N. P. *Science* **1996**, *274*, 948–953.
(17) Fujii, H.; Noda, K.; Asami, Y.; Kuroda, A.; Sakata, M.; Tokida, A. *Anal. Biochem.* **2007**, *366*, 131–136.
(18) White, P. J.; Squirrell, D. J.; Arnaud, P.; Lowe, C. R.; Murray, J. A. *Biochem. J.* **1996**, *319* (Pt 2), 343–350.
(19) Dukhovich, A.; Sillero, A.; Sillero, M. A. G. *FEBS Lett.* **1996**, *395*, 188–190.
(20) Chiu, M. I.; Katz, H.; Berlin, V. *Proc. Natl. Acad. Sci. U.S.A.* **1994**, *91*, 12574–12578.
(21) Chen, J.; Zheng, X. F.; Brown, E. J.; Schreiber, S. L. *Proc. Natl. Acad. Sci. U.S.A.* **1995**, *92*, 4947–4951.
(22) Brown, E. J.; Albers, M. W.; Shin, T. B.; Ichikawa, K.; Keith, C. T.; Lane, W. S.; Schreiber, S. L. *Nature* **1994**, *369*, 756–758.
(23) Banaszynski, L. A.; Liu, C. W.; Wandless, T. J. *J. Am. Chem. Soc.* **2005**, *127*, 4715–4721.
(24) Luker, K. E.; Smith, M. C.; Luker, G. D.; Gammon, S. T.; Piwnica-Worms, H.; Piwnica-Worms, D. *Proc. Natl. Acad. Sci. U.S.A.* **2004**, *101*, 12288–12293.
(25) Czarna, A.; Popowicz, G. M.; Pecak, A.; Wolf, S.; Dubin, G.; Holak, T. A. *Cell Cycle* **2009**, *8*, 1176–1184.

Tetrahedron Letters xxx (2013) xxx–xxx

Contents lists available at SciVerse ScienceDirect

Tetrahedron Letters

journal homepage: www.elsevier.com/locate/tetlet

Glycosylation of alcohols using glycosyl boranophosphates as glycosyl donors

Shiro Tatsumi, Fumiko Matsumura, Natsuhisa Oka, Takeshi Wada *

Department of Medical Genome Sciences, Graduate School of Frontier Sciences, The University of Tokyo, 5-1-5 Kashiwanoha, Kashiwa, Chiba 277-8562, Japan

ARTICLE INFO

Article history:
Received 26 February 2013
Revised 4 April 2013
Accepted 9 April 2013
Available online xxxx

Keywords:
Glycosylation
Boranophosphate
Glycosyl donor
Trityl cation
Oligosaccharide

ABSTRACT

A novel glycosylation that uses glycosyl boranophosphate triesters as glycosyl donors and trityl cation (Tr^+) as an activator was developed. Two types of reactions were studied: (1) the boranophosphate triester was activated with $TrNTf_2$ to react with an alcohol and (2) *O*-trityl ethers worked as both glycosyl acceptors and Tr^+ sources. The latter gave better results and the desired *O*-glycosylation products were rapidly generated and isolated in moderate to good yields.

Glycosyl phosphate triesters and their analogs are known to work as glycosyl donors and have been successfully applied to the synthesis of oligosaccharides.[1,2] One of their significant features is that their reactivity can be tuned by modifying the anomeric phosphate group.[3,4] Since glycosyl donors that can be specifically activated in the presence of another kind of donor are useful to simplify the synthesis of complex oligosaccharides and glycoconjugates,[5] various kinds of glycosyl phosphate analogs have been developed. However, the development of glycosyl phosphate analogs that are 'orthogonal' to each other is still a challenging task, and only a few kinds of such glycosyl phosphate derivatives have been reported to date.[4]

On the other hand, we have recently found that glycosyl boranophosphate derivatives,[1c,6,7] in which the P=O moiety of glycosyl phosphate triesters is replaced by a $P\rightarrow BH_3$ group,[8] have rather unusual properties for a glycosyl phosphate analog. Thus, glycosyl boranophosphate triesters are fairly stable in the presence of a Lewis acid, which can easily activate the corresponding glycosyl phosphite and phosphate triesters.[7a] Moreover, the glycosyl boranophosphate derivatives were found to undergo unique reactions. Since we had found that glycosyl boranophosphate diesters were smoothly converted into the corresponding glycosyl *H*-phosphonate diesters by treatment with a trityl cation (Tr^+) (Scheme 1, upper),[1c,7a,c] we also treated a glycosyl boranophosphate triester (**1**) with $TrClO_4$ in the presence of 4-*tert*-butylcyclohexanol to find that the mixture gave the glycosylation product. It is likely that Tr^+ oxidatively activated **1** to generate an active intermediate having a P^+ moiety, which then acted as a glycosyl donor, though this reaction mechanism is still hypothetical (Scheme 1, lower). We considered that the glycosyl boranophosphotriesters with such properties might be useful as glycosyl donors orthogonal to other kinds of glycosyl phosphates. We describe herein preliminary results of our study on the development of novel glycosylation reaction using the glycosyl boranophosphotriesters as donors.

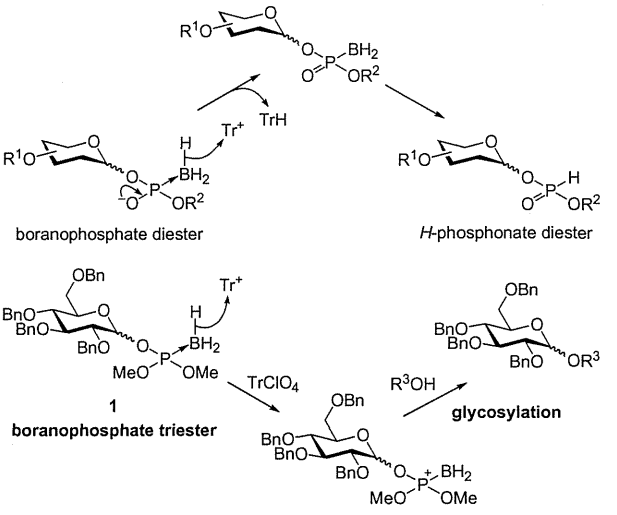

Scheme 1. Reactions of Tr^+ with glycosyl boranophosphate diester (upper) and triester (lower). R^3OH = *trans*-4-*tert*-butylcyclohexanol.

* Corresponding author. Tel.: +81 4 7136 3611.
E-mail address: wada@k.u-tokyo.ac.jp (T. Wada).

0040-4039/$ - see front matter © 2013 Elsevier Ltd. All rights reserved.
http://dx.doi.org/10.1016/j.tetlet.2013.04.032